https://doi.org/10.5194/egusphere-2025-4880
Preprint. Discussion started: 12 November 2025

Hybrid forest disturbance classification using Sentinel-1 and inventory data: a case-study for Southeastern USA

Franziska Müller[1,2], Laura Eifler[1,2], Felix Cremer[2], Pieter Beck[3], Gustau Camps-Valls[4], and Ana Bastos[1,2]

[1]Institute for Earth System Science and Remote Sensing, University Leipzig, Talstr. 35, 04103 Leipzig, DE
[2]Max-Planck Institute of Biogeochemistry, Dept. of Biogeochemical Integration, Hans-Knöll-Straße 10, 07745 Jena, DE
[3]European Commission, Joint Research Centre, Ispra, Italy
[4]Universitat de València, C/ Cat. Agustín Escardino Benlloch, 9 46980 Paterna, València, Spain

Correspondence: Franziska Müller (franziska.mueller@uni-leipzig.de)

Abstract.

Forest ecosystems are increasingly threatened by disturbances such as fires, droughts, storms, and insect and pathogen outbreaks. Accurate and timely disturbance mapping is essential for understanding their dynamics and informing mitigation strategies to combat widespread forest decline. Traditional inventories, such as the U.S. Forest Service's Insect and Disease Survey (IDS), provide detailed information on biotic and abiotic disturbances; however, they have varying coverage and inherent uncertainties in disturbance location, extent, and timing due to data collection constraints. Other approaches, such as satellite remote sensing, can in principle overcome some of these challenges by providing large-scale coverage and continuous spatio-temporal observations. However, robust classification algorithms need to be developed, which in turn require good-quality labels.

We present a novel approach for refining disturbance classification by combining IDS with Sentinel-1 radar backscatter change detection. The disturbed patches identified by Sentinel-1 are typically within 200–950 meters of IDS locations and generally agree on timing. When statistically examined against manual labels from PlanetScope, we found that S1DM performed better than IDS for wind and bark beetle disturbances, but not for defoliators. We find that Sentinel-1 tends to detect bark beetle disturbances earlier than IDS. We then combine spatial and temporal information about disturbance occurrence from Sentinel-1 change detection with information about the corresponding agent from IDS to produce a new high-quality forest disturbance reference dataset, Sentinel-1 Disturbance Mapping (S1DM), that can be used to develop remote sensing forest classification models.

Our approach highlights the benefits of combining satellite-based remote sensing with traditional aerial survey data, reducing costs associated with aerial surveys while providing a scalable method that can be adapted to various regions.

1 Introduction

Forests play a critical role in mitigating climate change by acting as carbon sinks and storing carbon in their biomass, such as leaves and roots, as well as in the soil (Pan et al., 2024). Recent observations suggest that climate change is likely contributing

https://doi.org/10.5194/egusphere-2025-4880
Preprint. Discussion started: 12 November 2025

to recent tree mortality events (Hartmann et al., 2022; Bauman et al., 2022; Hammond et al., 2022). Tree mortality is driven by a combination of natural disturbances (e.g., wildfires, storms, insects and pathogens) (Schuldt et al., 2020; Senf et al., 2020; Hicke et al., 2016, 2020; Kautz et al., 2017; Anderegg et al., 2015) and changes in land management, both of which can undermine forests' capacity to act as carbon sinks (Winkler et al., 2023; Harris et al., 2016, 2012; Nabuurs et al., 2013; Korosuo et al., 2023). In some cases, disturbances induce temporary carbon sources, contributing to amplify global carbon emissions (Kurz et al., 2008; Hicke et al., 2012; European Environment Agency (EU body or agency), 2024; Byrne et al., 2024).

As climate change accelerates, the frequency and intensity of disturbances, including wildfires (Canadell et al., 2021; Jones et al., 2022), storms (Senf and Seidl, 2021b), and insects and pathogens (Graziosi et al., 2020; Seidl et al., 2017), are increasing and heightening forest vulnerability (Forzieri et al., 2021; Altman et al., 2024). These changes in disturbance regimes pose risks to vital ecosystem services, including carbon sequestration, water regulation, soil protection, and biodiversity conservation that are critical for environmental and societal well-being (McDowell et al., 2020; Richter et al., 2022; Trumbore et al., 2015; Seidl et al., 2014; Thom and Seidl, 2016).

Despite the growing impact of forest disturbances on ecosystems worldwide, understanding their dynamics remains challenging due to the uneven global distribution of forest disturbance data (Kautz et al., 2017). A common approach to monitoring forest disturbances is through inventories, where trained surveyors document disturbances across large forested areas (McDowell et al., 2020; Coleman et al., 2018). However, the quality and extent of reporting vary significantly across regions. From 2002 to 2016, insect disturbance reports covered 98% of forested areas in North and Central America and 86% in Europe, but only 45% in Asia, according to the Food and Agriculture Organization (FAO, 2020). Coverage for severe weather disturbances was more limited, affecting 50% of forest areas in North America, 86% in Europe, and just 8% in Asia. This disparity highlights the uneven spatial coverage and inconsistencies in the types of natural disturbances recorded in inventory data.

While many inventories have limitations in terms of spatial and temporal coverage, some notable efforts provide more comprehensive datasets. Notable inventories include the Forest Service's Insect & Disease Detection Surveys (IDS) and the Canadian Forest Service's National Forestry Database (NFD), both relying on Aerial Surveys to monitor large-scale disturbances such as insects, diseases, wildfires, and droughts. In Europe, critical datasets on forest damage from insects and diseases include the Database of Forest Disturbances in Europe (Patacca et al., 2021, DFDE), the Dataset of Wind Disturbances in European Forests (Forzieri et al., 2020, FORWIND), and the Database of European Forest Insect and Disease Disturbances (Forzieri et al., 2020, DEFID2), with variable coverage in space and time. However, inventory data are affected by human errors, low sampling frequency, spatial inaccuracies, and inconsistencies in collection methods and definitions across countries, leading to spatial biases and challenges for dataset aggregation, preventing broader harmonized assessments (**?**McConnell, 2000; Coleman et al., 2018; Eifler et al., 2024; Forzieri et al., 2023).

Due to the limited and uneven distribution of traditional forest inventory datasets (Kautz et al., 2017; FAO, 2020), remote sensing has emerged as a crucial alternative for monitoring forest disturbances. Remote sensing provides a spatially and temporally consistent and cost-effective solution for tracking forest conditions across large areas and extended periods, with long-running satellite missions and sensors for example MODIS (Justice et al., 1998), Landsat (Markham and Helder, 2012;

https://doi.org/10.5194/egusphere-2025-4880
Preprint. Discussion started: 12 November 2025

Hansen and Loveland, 2012), and, more recently, the Sentinel fleet. Satellite time series of vegetation-related variables have allowed for the detection of forest disturbances, monitor forest cover changes (Hansen et al., 2013; Popp et al., 2020), and assess disturbance and regrowth patterns caused by wildfires, drought, and logging (Seidl and Turner, 2022; Senf et al., 2019; Heinrich et al., 2021; Senf and Seidl, 2021a), leading to global disturbance maps for these agents (Chuvieco et al., 2018; Vicente-Serrano et al., 2013; Curtis et al., 2018). In contrast, comprehensive mapping and classification of other disturbance agents, such as wind-throw or insects and pathogens outbreaks, remains limited, despite their known potential to cause substantial changes to forest ecosystems (Harris et al., 2016; Kautz et al., 2018, 2017). Global satellite-based estimates of forest disturbances caused by wind storms or biotic agents, such as insect outbreaks, currently do not exist (FAO, 2020; Kautz et al., 2017). This is primarily due to the difficulty in detecting smaller or slower disturbances—like droughts or subtle, temporary impacts from defoliators—where trees may recover after the event, making the damage harder to capture (McDowell et al., 2015). However, regional case studies have shown that it is possible to detect individual wind-throw events, bark beetle outbreaks, and defoliator attacks using existing satellite sensors such as Sentinel-2, Landsat, or MODIS (Negrón-Juárez et al., 2018; Senf et al., 2015; Eklundh et al., 2009; Meddens et al., 2012). Optical sensors provide extensive multispectral data, enabling the detection of disturbance hotspots, canopy health decline, and recovery across large areas (Senf and Seidl, 2018; Candotti et al., 2022; Hall et al., 2016; Hicke et al., 2016). However, their reliance on cloud-free conditions and limitations to detect subtle disturbances—such as those induced by biotic stress or drought (McDowell et al., 2015)—can limit the range of their applications.

An alternative solution is provided by Radio Detection and Ranging (RADAR) and Light Detection and Ranging (LiDAR) sensors, which offer information on structural changes. Radar imaging at high temporal and spatial resolution provided by the Sentinel-1 mission has shown potential for detecting different types of forest disturbances in regional case studies, including windthrows (Rüetschi et al., 2019), defoliation events (Bae et al., 2022), and bark beetle infestations (Dalponte et al., 2024). Since radar operates in the microwave range, it is not affected by cloud cover, making it particularly useful for continuous monitoring in all weather conditions. Furthermore, radar back-scatter is sensitive to changes in vegetation water content (Konings et al., 2021), and thus potentially more suitable to detect early states of slow-onset disturbances, such as insect outbreaks, and changes in canopy structure, driven for example by windthrow events.

Increasingly, remote sensing studies employ Artificial Intelligence (AI) techniques, to detect, map, and classify forest disturbances, demonstrating their ability to capture complex patterns (Andresini et al., 2024; Bárta et al., 2021; Hawryło et al., 2018; Gibson et al., 2020). Machine learning (ML) and deep learning (DL) are AI approaches that enable computers to learn from data. ML relies on algorithms that require pre-processed data with manually defined features, while deep learning uses neural networks with many layers to extract features from raw, unstructured data automatically. Unlike traditional ML, DL models do not require manual feature engineering, as the network identifies the most relevant patterns through the layers. Deep learning models, however, require vast amounts of labeled data to train effectively. Labels are ground-truth annotations where experts classify and mark specific features or disturbances in the data. The quality and accuracy of these labels have a direct impact on the performance of deep learning models. Unfortunately, generating these labels is a labor-intensive and costly process.

https://doi.org/10.5194/egusphere-2025-4880
Preprint. Discussion started: 12 November 2025

For forest disturbances, expert knowledge is needed to differentiate between various disturbance types, such as biotic stress, drought, or insect infestations. One potential solution to the data labeling challenge is leveraging legacy datasets, such as those from past forest inventory programs or remote sensing studies. These datasets could provide valuable resources for training deep learning models, reducing the need for new, manually labeled data. However, these legacy datasets are not yet fully reliable for this purpose. They often contain inaccuracies and inconsistencies in their labels—such as misclassifying healthy trees as disturbed due to the limitations of visual interpretation in aerial surveys (Kautz et al., 2017). Furthermore, remote sensing-derived datasets often fail to detect subtle disturbances, such as defoliators or ~~drougth,~~ leading to biased or incomplete labels (McDowell et al., 2015). Many of these datasets are also region-specific and not publicly available, which limits their potential use for training and validating models across diverse regions. These limitations emphasize the need for a more standardized, large-scale, and widely accessible benchmark dataset with accurate disturbance labels. Such a dataset would enable consistent training, validation, and comparison of deep learning models across various regions and disturbance agents.

This study aims to develop a high-quality forest disturbance benchmark dataset that leverages the strengths of inventory and satellite remote sensing data, making it suitable for broader forest monitoring applications. Specifically, this dataset is designed to support the development of satellite-based models for detecting and classifying disturbances in large regions.

Specifically, we focus on three key disturbance types: Bark Beetle, Defoliators, and Wind. The selection of these disturbances was driven by both their ecological relevance and existing gaps in remote sensing applications. Insect-driven disturbances, particularly from bark beetles and defoliating insects, are among the most significant sources of natural forest damage and net carbon loss in the United States (excluding anthropogenic activities such as logging or land-use change) (Harris et al., 2016). Yet, despite their ecological and economic importance, these disturbances remain difficult to detect and differentiate using conventional remote sensing, as they cause more gradual and subtle canopy changes compared to the abrupt impacts of fire. To address this challenge, we investigate whether radar observations can improve detection and characterization of insect-related disturbances, leveraging radar's sensitivity to structural and moisture changes not easily captured by optical data. Including wind disturbances complements this focus, as windthrow events also lack consistent large-scale mapping products and produce canopy changes similar to insect outbreaks. Together, these three disturbance types allow us to evaluate radar's potential to fill critical gaps in existing remote sensing capabilities—particularly for insect-related forest disturbances.

To achieve this, we integrate radar data from Sentinel-1, which provides spatially and temporally continuous, cloud-penetrating, structural information, with the long-term, large-scale Insect & Disease Survey (IDS) inventory dataset that is available electronically for the entire USA since 1997. IDS offers detailed, aircraft-based disturbance observations, archiving methodologies, extensive temporal coverage, and detailed information about disturbance agents. As discussed above, IDS suffers from limitations inherent to aerial detection surveys, such as human error, inconsistent sampling, coverage gaps, and spatial inaccuracies (Forest Service U.S. Department of Agriculture, 2024; McConnell, 2000; Coleman et al., 2018; Eifler et al., 2024; FAO, 2020; Kautz et al., 2017). By combining the two datasets, we aim to leverage the IDS detailed mapping and disturbance agent information while overcoming the uncertainties in size, location, and timing of the disturbances through independent estimates based on change detection in the radar backscatter signal of Sentinel-1.

https://doi.org/10.5194/egusphere-2025-4880
Preprint. Discussion started: 12 November 2025

This approach enables us to refine traditional disturbance mapping and generate a reference dataset with higher spatial, temporal, and disturbance agent accuracy. This integration of inventory and remote sensing data creates a hybrid dataset, providing a semi-automatic approach to bridge information from different datasets and reduce spatial and temporal uncertainties, thereby supporting efforts to monitor diverse disturbance agents across vast regions.

2 Data

2.1 Study area

This study focuses on a specific region within the United States - the southeastern area classified by the United States Department of Agriculture (USDA) as Region 8 (Fig. 1). It spans approximately 73 million hectares of forest across 13 states, with a wide variety of forest types and disturbance regimes, making it an ideal area for studying forest dynamics and disturbances on a large scale. The forests in this vast region exhibit high diversity, with a mix of broadleaf and coniferous species flourishing across a spectrum of climate conditions. From the humid subtropical zones of coastal and lowland areas to the temperate mixed forests of higher elevations, these ecosystems support a rich array of ecological functions and forest management practices, each uniquely shaped by the interplay of climate, topography, and species composition. In the Interior Highlands and Interior Plains (the central and northern parts of the study area), low-elevation mountains and flat terrain are dominated by deciduous species, including White Oak (Quercus alba), Red Oak (Quercus rubra), and various Hickory species (Carya spp.). In contrast, the Atlantic Plains (southern regions), with their wetter conditions and extensive wetlands, support deciduous species like Baldcypress (Taxodium distichum), Water Tupelo (Nyssa aquatica), and Sweetgum (Liquidambar styraciflua). The Appalachian Highlands, with higher elevations and cooler climates, contribute further diversity, featuring mixed species like Sugar Maple (Acer saccharum), Yellow-poplar (Liriodendron tulipifera), and Eastern White Pine (Pinus strobus). A comprehensive species list is available in Appendix Table A1 and the US Forest Service Map for Tree Species in the Southeastern United States (Institute, US Forest Service - FIA Forest Types of the Southeastern United States).

This diverse forest composition, with varying ecological zones and differing management strategies—from conservation-driven national parks to privately managed timberlands—creates a complex landscape where disturbances manifest in various ways across the region. By not focusing on a single tree species or management practice, we conduct a complex yet holistic analysis of disturbances that can be applied to a wide range of forest types.

To analyze forest disturbances affecting this region, we utilize three key datasets: the Insect and Disease Survey (IDS), Sentinel-1 Change-Detection (S1CD), and Tree Canopy Cover (TCC) datasets. These datasets form the foundation of our analysis, providing complementary information on forest disturbances, structural changes in canopy cover, and the presence/absence of trees. Table 1 summarizes their key characteristics, with further details discussed in the following sections.

https://doi.org/10.5194/egusphere-2025-4880
Preprint. Discussion started: 12 November 2025

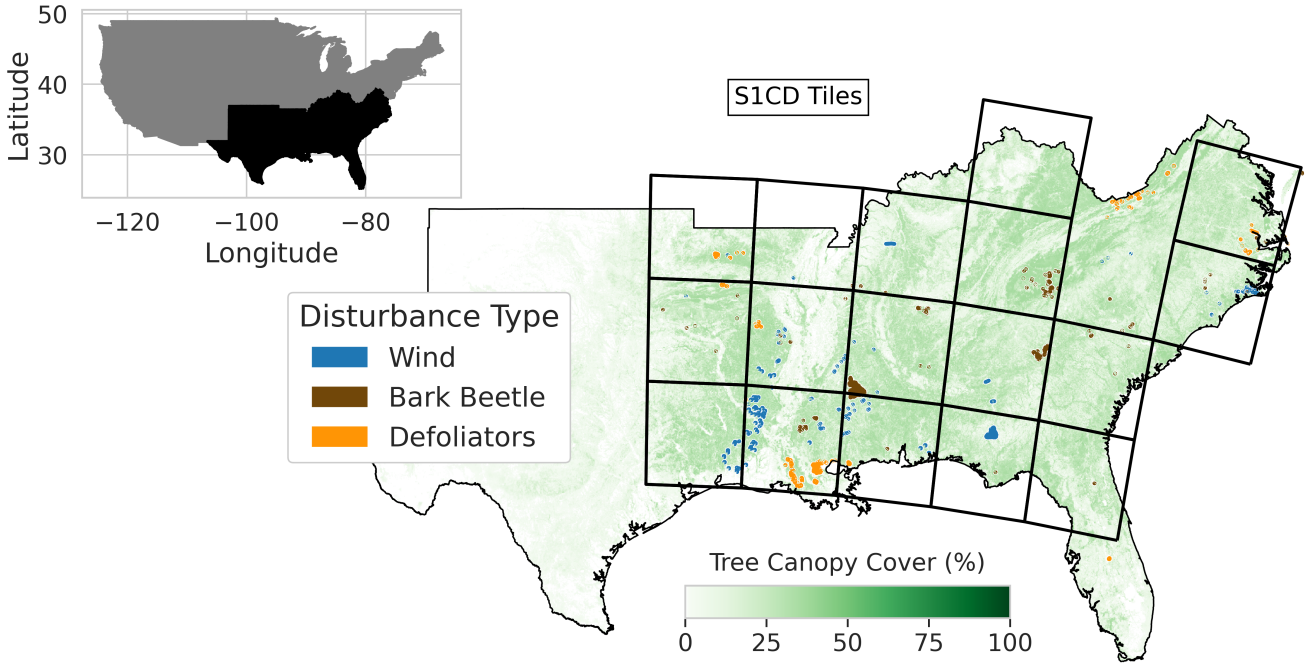

Figure 1. Spatial overview of USDA Region 8, with detailed disturbance and canopy cover data. The inset map (top left) shows the location of Region 8 within the United States, highlighted in black. The main map displays the outline of Region 8, with Tree Canopy Cover (TCC) for 2015 shaded in green, representing the percentage of canopy coverage. Overlaid on the TCC map are visually enlarged disturbance patches for three selected disturbance types (wind, bark beetles, and defoliators) based on preprocessed Insect and Disease Survey (IDS) data (Forest Service U.S. Department of Agriculture, 2024) from 2016 to 2020, showing disturbances under 15 km^2 in size. The grid outlines represent the spatial coverage of the Sentinel-1 Change-Detection (S1CD) dataset ((Cremer et al., 2020); this study). This figure illustrates the spatial distribution of tree canopy cover, disturbance events, and the S1CD grid tiles used for analysis across Region 8.

2.2 Insect and Disease Detection Survey (IDS)

The Insect and Disease Survey (IDS), conducted by the United States Department of Agriculture (USDA) Forest Service (Forest Service U.S. Department of Agriculture, 2024), monitors forest damage and mortality resulting from various disturbance agents. Since 1997, the IDS has monitored disturbance agents across the United States and its territories, including fires, wind, bark beetles, defoliating insects, and fungal diseases. Disturbances are mapped as geo-referenced polygons (or occasionally points) that represent areas where damage was observed, though not all trees within a polygon are necessarily affected. For each polygon, surveyors record the tree species affected, the causal agent (with over 1,000 selectable agents), the damage type (e.g., mortality, defoliation percentage, crown dieback, branch breakage, or other non-mortality damage), and the severity class, expressed as the percentage of live and damaged trees within the polygon (Very Light: 1–3% through Very Severe: >50%).

https://doi.org/10.5194/egusphere-2025-4880
Preprint. Discussion started: 12 November 2025

	IDS	S1CD	TCC
Information	Forest damage and mortality caused by various disturbance agents	Information of structural change on the earth's surface based on Sentinel 1	Tree canopy cover for CONUS in 2017
Data	Spatial data structured in points and polygons with associated attributes documenting forest health and disturbances.	Raster data in binary format (1s and 0s) indicating structural change status.	Raster data in GeoTIFF format representing tree canopy cover as a percentage.
Spatial resolution	~~0.5 m^2~~ - 62 231 km^2 polygons	20 x 20 m raster	30 x 30 m raster
Temporal availability	Yearly data since 1997	Yearly data from 2016 to 2021	2017

Table 1. Key characteristics of the datasets used in this study: the Insect and Disease Survey (IDS), Sentinel-1 Change-Detection (S1CD), and Tree Canopy Cover (TCC). This table summarizes the data type, format, spatial resolution, and temporal availability for each dataset, providing an overview of the input data used to assess forest disturbances and canopy changes across USDA Region 8.

Each record also contains metadata on survey year, region, observation ID, and survey method (e.g., aerial sketch mapping, remote sensing, or ground observations). Since 2020, survey protocols have included greater reliance on remote sensing due to COVID-19 restrictions, and flown survey extents and resulting polygons are made available annually as geodatabases. For consistency, this paper refers to this dataset as IDS.

In our study region 8, the IDS recorded a total of 2,992 disturbances from 2017 to 2020. Bark beetle outbreaks were the most frequent (1,177 events), followed by wind (478) and defoliators (213). Annual disturbance counts varied considerably, from 210 events in 2017 to 1,374 in 2018. The total disturbed area also varied by type and year: defoliation affected the most significant area in 2018 (119 km^2), while wind caused the largest area loss in 2020 (343 km^2). Bark beetle outbreaks were widespread but generally affected smaller areas per event, whereas wind and defoliation events often covered larger contiguous areas.

IDS data is collected primarily through aerial detection surveys (ADS) conducted by trained professionals. While ground-based surveys are used to verify specific disturbances or assess localized events, ADS provides the most effective method for large-scale disturbance monitoring, especially for extensive forest areas (Coleman et al., 2018).

Although mapping disturbances across large areas, such as the United States, would be impossible without ADS, this method presents several challenges. Surveyors must contend with factors such as the aircraft's high speed (approximately 100 mph), the angle of observation, and the complexity of detecting disturbances in a constantly changing landscape. Despite the aid of geo-referencing tools, these challenges often result in imprecise delineations, sometimes including healthy trees or non-forest

https://doi.org/10.5194/egusphere-2025-4880
Preprint. Discussion started: 12 November 2025

areas, especially during large-scale outbreaks when time constraints limit accuracy (Backsen and Howell, 2013; Coleman et al., 2018; Kautz, 2014). This uncertainty is explicitly acknowledged in the IDS protocol: for each mapped polygon, the attribute percent affected provides a standardized estimate of the proportion of trees within the area that the identified disturbance agent impacts. Although quick decisions are necessary during ADS, surveyors generally attribute disturbance agents correctly, making false positives (Type I errors, where a disturbance is recorded but did not actually occur) rare. However, in the case of compound disturbance events i.e., events that occur in quick succession, simultaneously, or that trigger one another (e.g., a drought increasing bark beetle activity, or the Vaia storm followed by bark beetle outbreaks), overlapping influences can make it difficult to disentangle individual agents, sometimes leading to false negatives (Type II errors, where a real disturbance impact is missed or misattributed), resulting in specific disturbance effects going unnoticed (Coleman et al., 2018).

Biotic disturbances, such as defoliators and bark beetles, occur within specific activity windows that must be captured accurately through timely ADS. However, weather, funding, and surveyor availability can delay flights, preventing surveys from being conducted during these critical windows. As a result, disturbances may be missed or monitored at suboptimal times (McConnell, 2000). Additionally, some disturbances may not be detectable until after they occur, resulting in a time lag between the actual disturbance and its detection, as seen with bark beetles (Kautz, 2014). Due to the large areas that must be covered, flight patterns often change from year to year, and some regions may not be surveyed at all in a given season. Survey coverage follows specific flight paths rather than encompassing every forested area, and the extent of the flown area is made available annually as a geodatabase. This information is particularly important for interpreting records from 2020 and 2021, when COVID-19 restrictions limited aerial surveys and protocols shifted toward greater use of remote sensing. This variability in flight coverage can introduce biases and inconsistencies, particularly in disturbance attribution, since areas may not always be flown at the optimal time for detecting damage.

Given these spatial and temporal uncertainties, ground verification is used to validate aerial survey data and investigate anomalies. However, due to time, funding, and data volume constraints, less than 1% of the mapped polygons are verified annually (Coleman et al., 2018).

Despite these challenges, the IDS dataset offers invaluable insights into large-scale forest disturbances. With nearly 27 years of data since 1997, it provides a unique perspective for analyzing short- and long-term disturbance patterns. Another strength is its broad spatial extent, spanning the entire United States, including remote and difficult-to-reach areas where ground-based monitoring is impractical. Importantly, it covers both public and private lands, thereby reducing biases related to forest management practices, land ownership, and tree species. The dataset captures a wide range of disturbance agents, including fires, wind, bark beetles, defoliating insects, and fungal diseases, along with detailed metadata on damage severity, affected tree species, and other critical factors. While it has limitations in spatial and temporal accuracy and verification, its extensive coverage, variety of disturbance agents, and detailed metadata make it an indispensable tool for understanding forest dynamics and disturbance patterns across the United States.

https://doi.org/10.5194/egusphere-2025-4880
Preprint. Discussion started: 12 November 2025

2.3 Tree Canopy Cover (TCC)

To focus exclusively on forested areas, we used the Tree Canopy Cover (TCC) dataset from the U.S. Forest Service's Geospatial Technology and Applications Center, available for CONUS for the years 2015–2020 (https://data.fs.usda.gov/geodata/rastergateway/treecanopycover/, accessed 18 September 2025) at a 30 m × 30 m spatial resolution and used to distinguish forested areas from non-forest areas in the study.

2.4 Sentinel-1 Change Detection (S1CD)

Here, we aim to produce an independent, satellite-based dataset of forest disturbances using Sentinel-1 C-Band Synthetic Aperture Radar (SAR) data. Unlike optical sensors, SAR is unaffected by cloud cover or sunlight, allowing consistent, year-round monitoring at high temporal (12-day) and spatial (30 m) resolution. C-band radar (5.4 GHz, 5.6 cm wavelength) is primarily sensitive to canopy water content and upper-canopy structure, making it well suited to capture fine-scale changes in forest condition. Bark beetle outbreaks reduce canopy moisture, defoliators minimize leaf area, and wind can remove branches or uproot entire trees, creating gaps and altering canopy structure—all of which can be detected by radar even when foliage remains green to human observers or spectral satellite sensors. This sensitivity enables us to assess the extent to which Sentinel-1 can detect these types of disturbances and how changes in canopy structure and moisture translate into observable radar signals.

To detect disturbed patches, we follow the method described by (European Commission. Joint Research Centre., 2023) (Section 3.3). To adapt this method to our study, we use Sentinel-1 data at 12-day time-steps from 17 tiles covering our study region for the period 2016–2021 (see Figure 1, Table A2). Before our analysis, the data was adjusted to account for terrain variations (Wagner et al., 2021) and rescaled to a 20 m × 20 m resolution. Finally, the data was mapped onto the EQUI7 grid system (Bauer-Marschallinger et al., 2014) for consistency and ease of analysis.

2.5 PlanetScope

PlanetScope imagery used in this study was accessed through the Planet Education and Research (E&R) Standard Program (PBC), which provides limited, non-commercial access to PlanetScope and RapidEye imagery for university-affiliated students, faculty, and researchers. Access to the program requires a valid university email address; in this case, imagery was obtained using an institutional email from the University of Leipzig, granting permission to use PlanetScope data for research purposes.

PlanetScope imagery consists of high-resolution optical data acquired from a constellation of CubeSats, with a nominal daily revisit, although actual coverage can be affected by clouds, acquisition gaps, or satellite scheduling. Each scene has a spatial resolution of approximately 3–5 m and includes four spectral bands: Blue, Green, Red, and Near-Infrared, suitable for monitoring vegetation and detecting forest disturbances.

RapidEye imagery complements PlanetScope with 5 m multispectral data, including a Red Edge band in addition to Blue, Green, Red, and Near-Infrared, enhancing vegetation health assessment. Both datasets are orthorectified and radiometrically

https://doi.org/10.5194/egusphere-2025-4880
Preprint. Discussion started: 12 November 2025

calibrated, allowing consistent analysis over time and across study areas. Their high temporal frequency and spectral information make them particularly useful for tracking fine-scale forest disturbances and vegetation dynamics.

3 Methods

The flowchart in Figure 2 outlines the key steps involved in preprocessing, intersecting, and analyzing the data, which are explained in more detail below. All processing was done using Python (see Code Availability).

Throughout this paper, we follow consistent terminology when referring to spatial representations of disturbances. We use the term *polygon* to describe the vector-based geometries in the IDS dataset, reflecting the original IDS data format and nomenclature. In contrast, *patch* refers to the disturbance outlines derived from the S1CD dataset in raster format, which are later converted to polygons for analysis.

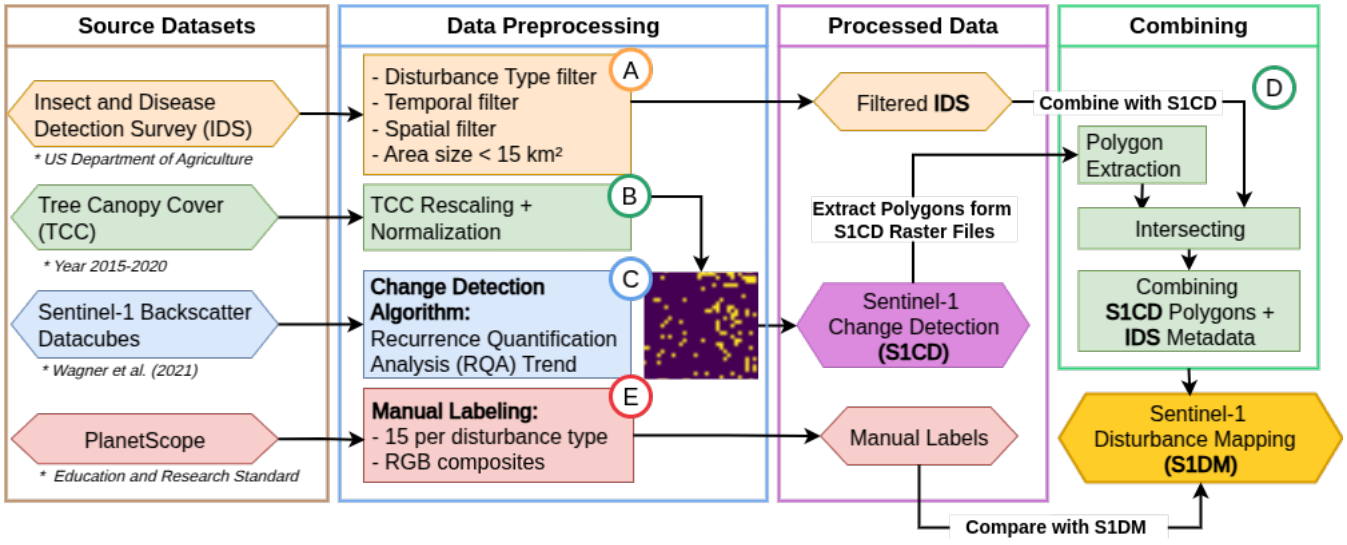

Figure 2. Workflow illustrating the methodology used to create the radar-enhanced dataset and analyze the results. Rectangles represent processes or functions (data transformations), while hexagons represent datasets. The main processing steps include: a) Preprocess IDS dataset to filter and prepare disturbance polygons for analysis; b) Preprocess the TCC dataset to standardize tree canopy cover information; c) Apply the Sentinel-1 SAR Change Detection algorithm to identify disturbed patches; d) Intersect and combine IDS and Sentinel-1 Change Detection (S1CD) datasets to obtain the final S1DM dataset; e) Acquire and manually label PlanetScope (Education & Research Standard) data to statistically compare size and shape of disturbances with the IDS and S1DM dataset.

3.1 IDS Preprocessing

The original IDS dataset provided extensive detail, including 47 metadata variables that captured information such as disturbance agents, host tree species, severity of damage, disturbance year, tree mortality rates, and other contextual details. However, the complete list of these details was beyond the scope of our analysis. At the very beginning of our preprocessing pipeline,

https://doi.org/10.5194/egusphere-2025-4880
Preprint. Discussion started: 12 November 2025

we restricted the analysis to areas that IDS actually surveyed; disturbances reported by other datasets (e.g., S1CD) outside the flown extent were ignored. Following the approach outlined by Eifler et al. (2024), we implemented several preprocessing steps to clean, simplify, and streamline the data, thereby aligning it more closely with our research needs.

We focused on events within the study area (USDA Region 8) and analyzed disturbances from 2016 to 2020. This period aligned with the availability of Sentinel-1 data (launched in 2014, with data available from 2016 onwards). Furthermore, our analysis focused on three specific types of disturbances: wind, bark beetles and defoliators. To select the disturbances of interest, we extracted 11 key variables from the IDS metadata. The damage-causing agent (DCA_ID, DCA_CODE) is recorded both as text and as a numerical code, representing agents such as wind, bark beetle, or defoliators. The survey year (SURVEY_YEA) indicates when the disturbance was observed, and the region (REGION_ID) specifies the location within USDA Regions. The damage type (DAMAGE_TYP, DAMAGE_T_1) is recorded as both a text description (e.g., defoliation, mortality, crown dieback) and a numerical code. The percentage of affected trees (PERCENT_AF) indicates the proportion of trees within the polygon that were damaged, while the host species (HOST, HOST_CODE) identifies the affected tree ~~type~~ in both text and numeric form. Finally, the geometry variable defines the spatial extent of the affected area. Together, these variables allowed us to identify disturbance agents, quantify the extent of damage, and link it to specific tree species across regions. Based on the 26 disturbance agents identified by IDS, we aggregated disturbances into "wind", "bark-beetle" and "defoliators". Following Eifler et al. (2024), we aggregated spatially overlapping polygons from the same survey year and disturbance category into single events (ID_E). To prioritize the most severe disturbances, more likely to be identified by satellite, we retained only those events classified as "Severe" or "Very Severe" (where more than 30% of trees were affected), as well as those with no entry for the percentage of affected trees (PERCENT_AF). According to Eifler et al. (2024), some IDS-reported polygons included predominantly non-forest areas, had irregular shapes, or spanned unrealistically large extents. Building on their approach of excluding events larger than 2000 km^2, we applied a stricter filter, excluding polygons larger than 15 km^2. Here, we did not use a tree canopy cover filter because, as mentioned in Section 2.2, the IDS had spatial location inaccuracies, and we did not want to exclude events that might have been spatially skewed but still relevant.

Forest disturbances often do not occur in isolation, as a given disturbance can influence or trigger another, e.g., a severe bark beetle infestation following a drought (Seidl et al., 2014). This is often found in the IDS data, where multiple polygons overlap in space and time. However, given our aim to develop a dataset that could be used as a reference to train forest disturbance classification models, we focused on disturbances that occurred independently, in order to capture a cleaner signal for each disturbance type. For this, we excluded spatially and temporally compounded events overlapping spatially with other disturbances within a ±5-year window to eliminate spatially and temporally compounded events. We kept overlapping events with the same disturbance type, likely indicating a continuous event.

3.2 Tree Canopy Cover

To focus our analysis on forested areas, we first processed the Tree Canopy Cover (TCC) dataset for the years 2015–2020. The original 30 m × 30 m raster was resampled to 20 m × 20 m using nearest-neighbor interpolation to ensure consistency with

https://doi.org/10.5194/egusphere-2025-4880
Preprint. Discussion started: 12 November 2025

the Sentinel-1 SAR data. The dataset was then reprojected to the EPSG:4326 coordinate reference system and clipped to the boundaries of the study region, excluding areas outside the region.

Pixel values in the TCC dataset range from 0 to 255, representing scaled canopy cover percentages (0 = 0%, 255 ≈ 100%). We normalized the values to a 0–1 range for further processing. For each year from 2015 to 2020, the TCC data were used to mask the following year's Sentinel-1 SAR files: pixels with TCC ≥ 30% were classified as forested, while pixels below this threshold were considered non-forest.

3.3 Creation of Sentinel-1 Change Detection (S1CD)

As described in Section 2.4, we created an independent satellite-based dataset of forest disturbances using Sentinel-1 SAR data. A total of fifteen tiles covering the study region from 2016 to 2021 were used.The data were rescaled to 20 m × 20 m resolution, mapped onto the EQUI7 grid, and adjusted for topography. This preprocessing produced topographically corrected, orthorectified γ backscatter rasters, ready for time series analysis.

Building on this data, we applied the pixel-wise change detection method described by European Commission. Joint Research Centre. (2023) to identify and analyze forest disturbances. For each preprocessed Sentinel-1 Tile, we detected land-cover changes within a given year by considering a time series spanning from July of the previous year to June of the following year, thus covering a two-year window. Changes detected within this time window were attributed to transitions occurring in the central calendar year. However, this approach introduced some temporal uncertainty, as disturbances occurring within the ±0.5-year buffer around the center year could also be included. While this method improved the detection robustness, some changes may not have aligned perfectly with the central calendar year, reflecting an inherent limitation in temporal attribution. At the end of this step, we had pixel-wise time series.

We applied Recurrence Quantification Analysis (RQA) to each pixel individually to quantify the similarity between time steps in the series.This algorithm is schematically illustrated in Appendix A2. In brief, the method plots the time series against itself to generate a Recurrence Plot (RP), where the main diagonal (x = 0) shows a perfect match as each time point correlates with itself. Following (Cremer et al., 2020), we computed the Recurrence Rate (RR) for each diagonal, defined as the fraction of recurrent points along the diagonal relative to its length. Plotting RR across diagonals produces a recurrence line, and the slope of this line reflects the temporal dynamics of the pixel: a slope of zero indicates no change, whereas negative or positive slopes indicate decreasing or increasing recurrence, respectively. Pixels with a RQA-Trend value below the threshold of -1.28 were considered to show no significant change. In contrast, values above this threshold were classified as indicating a change in that specific year. This process produced a binary raster, where each pixel indicated whether a structural change in forest cover occurred during the analyzed year.

The resulting raster was projected into the WGS84 coordinate system (EPSG:4326) to ensure greater compatibility with other spatial datasets. To exclude non-forest areas from the raster, we used the preprocessed CONUS Tree Canopy Cover (TCC) dataset to filter out non-forest areas (refer to 3.2). Lastly, we converted the binary raster pixels into polygons to ensure a consistent polygon-based format for the dataset. In the following, we referred to this dataset as S1CD (Sentinel-1 Change Detection).

https://doi.org/10.5194/egusphere-2025-4880
Preprint. Discussion started: 12 November 2025

3.4 Sentinel 1 Disturbance Map (S1DM)

The two datasets — the IDS and the yearly change detection via S1CD — provided complementary and independent information on forest disturbances and their causes. First, we compared the two datasets spatially and temporally to identify the S1CD disturbed patches that best corresponded to the reported IDS disturbances. To focus on enhancing disturbance information rather than detecting new events, we only considered S1CD elements located within a buffer around IDS polygons, excluding all areas outside both the buffer and the flown survey paths. With this, we aimed to extract a subset of disturbed patches that could be enhanced with information on disturbance agents from IDS. To account for spatial uncertainty in the aerial survey data (Eifler et al., 2024), we tested buffer distances from 100 to 1,000 meters, and selected 500 meters as the optimal balance between retaining relevant events and minimizing noise. Accordingly, a 500-meter buffer was applied around each IDS event. To account for the inherent temporal uncertainties in the IDS and S1CD datasets, we used a temporal buffer of ± 2 years for the S1CD data. This was necessary because the Sentinel-1 change detection algorithm introduces a ± 0.5-year uncertainty due to its time window from July of the previous year to June of the following year (Section 3.3). Additionally, Eifler et al. (2024) reported a ± 1.1-year uncertainty in the disturbance years recorded in the IDS dataset compared to forest inventory data (FIA). Considering these overlapping uncertainties, we opted for a ± 2-year buffer to achieve a more reliable temporal alignment between the two datasets.

We then intersect both the IDS and S1CD datasets (see Figure A2. We restricted our analysis to areas along the flight paths of the survey, where IDS data were available. Since multiple S1CD patches could overlap with a single IDS disturbance, we treated these as scattered patterns from the same event and combined them into one unified multi-polygon. Following this, we excluded any aggregated disturbances larger than 15 km^2, aligning the S1CD-derived dataset (S1DM) with the same size threshold used for the IDS dataset. Thus, we focused our analysis on small—to medium-sized disturbances.

The resulting dataset, **Sentinel 1 Disturbance Mapping (S1DM)**, contains all disturbed patches detected by Sentinel-1 that align with IDS-recorded disturbances in space and time, given the uncertainty considered.

Each disturbance event is represented as a separate entry in a GeoDataFrame. Table A3 provides the structure and attributes of the dataset. Events spanning multiple years are linked based on spatial adjacency and continuity of the affected area, with all related entries assigned the same event ID (IDX_D). Recording each year separately allows us to track temporal changes in shape and extent. This system enables us to track the evolution of each event in both time and space, providing valuable insights into its changes throughout its duration.

To assess the spatial agreement between IDS and S1DM, we first analyzed the direct overlap of polygons without applying the 500 m buffer used in previous alignment steps. For each disturbance type (Figure 4), we calculated: a) the percentage of IDS polygons covered by S1DM, calculated as $\text{Percentage} = \frac{A(\text{IDS} \cap \text{S1DM})}{A(\text{IDS})} \times 100$, and b) the percentage of S1DM polygons that overlap with IDS, expressed as $\text{Percentage} = \frac{A(\text{IDS} \cap \text{S1DM})}{A(\text{S1DM})} \times 100$

To complement this, we also examined the spatial characteristics of individual S1DM disturbances compared to IDS (without buffer) (Figure **??**). For this, we calculate three key metrics - the disturbance area, the convex hull area, and the centroid distance — to quantify the spatial characteristics of the disturbances in S1DM and compare them to the IDS dataset. The disturbance

https://doi.org/10.5194/egusphere-2025-4880
Preprint. Discussion started: 12 November 2025

area A_D represents the actual size of each detected patch, providing a direct measure of the affected region. While IDS records each disturbance as a single contiguous patch, disturbances in S1DM often consist of multiple smaller, scattered polygons forming a multipolygon. To account for this, we compute the convex hull area A_{CH}, which encloses all individual polygons of an S1DM disturbance within the smallest possible convex boundary. This metric helps us understand the overall spatial spread of an event, providing insight into how disturbances extend spatially compared to IDS. To examine spatial alignment between IDS and S1DM polygons, we calculate the centroid distance $\Delta_{centroid}$, defined as the Euclidean distance between the centroids ($C_P = (x_C, y_C)$)of corresponding polygons in the two datasets. These metrics enable us to evaluate differences in size, shape, and spatial positioning between IDS and S1DM disturbances, providing insights into the degree of alignment between the two datasets in terms of scale and location.

3.5 Verification with PlanetScope Data

We compared the original IDS dataset with our new S1DM dataset to evaluate whether integrating Sentinel-1 data improved the spatial accuracy and boundary delineation of disturbance events. To further validate the precision of S1DM, we used PlanetScope for spatial verification.

For this purpose, we selected 15 events per disturbance type where the disturbed areas could be clearly identified. We used imagery from the PlanetScope and RapidEye satellite constellations (Planet Labs Education and Research Standard Account; accessed August–September 2025 (PBC)), acquired by the Dove satellites with four spectral bands (blue, green, red, and near-infrared), a nominal daily temporal resolution, and a spatial resolution of 3–5 m. Only images with less than 10 % cloud cover were selected to ensure clear visual interpretation. For each of these events, we then performed visual interpretation and delineated the disturbed areas.

While the visual interpretation was performed systematically, we acknowledge that it may carry subjective bias. For example, some events were recurrent, making it difficult to distinguish the original disturbance from subsequent changes such as regrowth, new tree line damage, or clear-cuts. To minimize these issues, we focused on extracting the disturbance outline as accurately as possible, emphasizing the largest and clearest extent of the natural disturbance prior to any clear-cut. For each event found in PlanetScope, we recorded the first disturbance date, any subsequent disturbance years, and, where applicable, the year of clear-cutting.

To quantitatively evaluate the spatial agreement between IDS and S1DM disturbance maps and manually delineated reference polygons, we computed two complementary metrics for each event. Manual polygons, visually validated using PlanetScope imagery, were considered the ground truth. For each polygon of IDS or S1DM, we computed the spatial overlap (Eq. 1) and the ~~Jaccard similarity~~ (Jaccard, 1902) (Eq. 2) with the corresponding manual polygon.

The overlap (O) is defined as the fraction of the manual polygon area covered by the candidate polygon, with values ranging from 0 to 100%, representing the overlap between the polygon areas:

$$O = \frac{|\mathbf{A}_{candidate} \cap \mathbf{A}_{manual}|}{|\mathbf{A}_{manual}|} \times 100, \quad (1)$$

https://doi.org/10.5194/egusphere-2025-4880
Preprint. Discussion started: 12 November 2025

The ~~Jaccard similarity index (J)~~ ranges from 0 (no overlap) to 1 (perfect match) and is calculated as:

$$\mathbf{J} = \frac{|\mathbf{A}_{\text{candidate}} \cap \mathbf{A}_{\text{manual}}|}{|\mathbf{A}_{\text{candidate}} \cup \mathbf{A}_{\text{manual}}|}, \tag{2}$$

To evaluate the performance of IDS and S1DM in capturing the spatial features of the disturbance events, we analysed the distributions of the spatial overlap and Jaccard similarity across samples for each disturbance type. Then one-sided paired t-tests were applied with a primary significance threshold of $\alpha = 0.05$ (denoted by *) and a secondary threshold of $\alpha = 0.1$ (+), to test the hypothesis that S1DM systematically better captured the spatial characteristics of the disturbance events (as identified by manual labelling) than IDS. RGB composites from PlanetScope imagery were generated to visually assess spatial correspondence between datasets. For each manually labeled event, the best available image after the earliest manually identified disturbance date was selected to represent disturbance conditions. Polygons corresponding to the manual labels, IDS, and S1DM were overlaid on these composites, illustrating the spatial extent and relative alignment of the detected disturbance areas.

For the temporal similarity, we examined all years in which disturbances could be detected in the PlanetScope data. In the case of Defoliators, this may include recurring attacks, while for Bark Beetle disturbances, the spread of the infestation can result in repeated detections. We also considered clear-cuts and recorded them as disturbance events when they followed natural hazard impacts. It should be noted that this analysis is subject to bias, as both the manual delineations and the IDS dataset are based on visual interpretation. The results, therefore, need to be interpreted with these limitations in mind.

4 Results

4.1 Spatial and temporal agreement of IDS and radar-based disturbance detection

Specifically, we assessed how many IDS disturbance events contained a corresponding S1DM signal within a 500 m buffer around each IDS patch. Figure 3 shows that the detection effectiveness of S1DM varies by disturbance type. Wind disturbances show the highest agreement with IDS, with only 1.9 % of IDS wind events not having a corresponding S1DM signal within the buffer. Bark beetle disturbances follow, with 76 % of IDS patches having a corresponding S1DM signal. In contrast, agreement is lower for defoliator disturbances, where only 67% of IDS disturbed areas have a corresponding S1DM signal within the 500 m buffer.

https://doi.org/10.5194/egusphere-2025-4880
Preprint. Discussion started: 12 November 2025

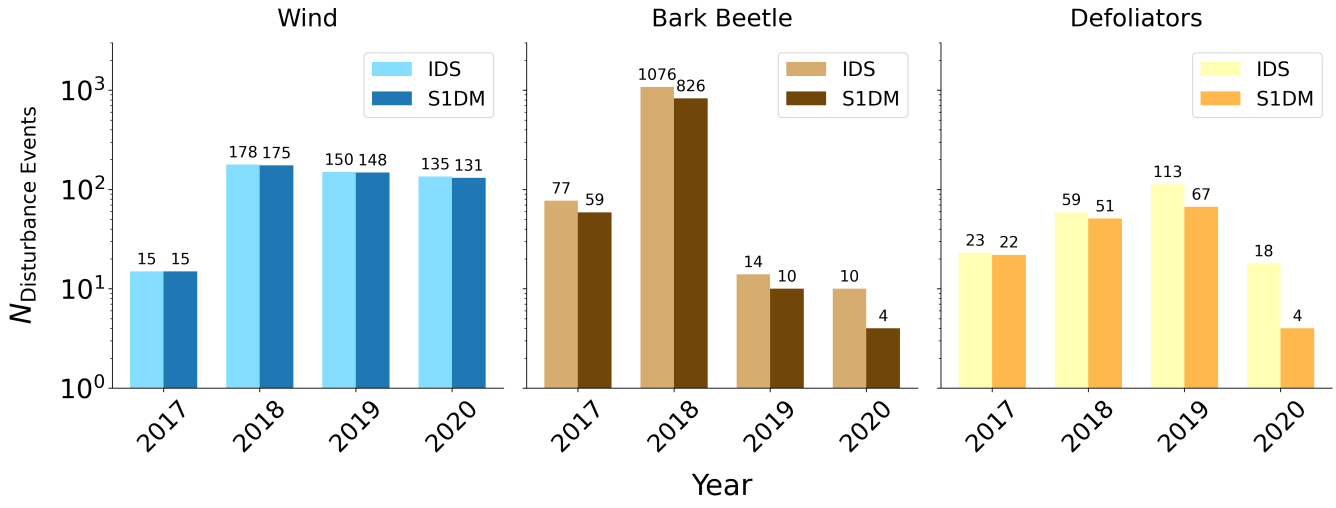

Figure 3. Detection efficiency of various disturbance types using Radar Change Detection. The bar plot shows the number of events on the y-axis (log scale) for each disturbance type on the x-axis, with IDS shown in light color and S1DM in darker color. The total number of IDS disturbance events that had a corresponding S1DM signal within the 500 m buffer was 469 for wind (S1DM: 469; IDS: 478), 899 for bark beetle (S1DM: 899; IDS: 1177), and 144 for defoliators (S1DM: 144; IDS: 213).

We analyzed the event size and the spatial position of S1DM in comparison to IDS (without buffer). To quantify this relationship, we examine the spatial agreement between IDS and S1DM for each disturbance type (Figure 4) by calculating a) the percentage of IDS polygons covered by S1DM and b) the percentage of S1DM polygons that overlap with IDS . When examining the overlap without buffer, we find that IDS is covered to a small extent by S1DM polygons, with median coverage across all disturbance types remaining below 10%. There is no overlap for most Bark Beetle events, and for all other disturbance types, IDS is covered by less than 16% of S1DM polygons in 50% of the cases. When examining S1DM polygons, the proportion of each polygon's area that overlaps with IDS is generally low for bark beetle and defoliator events. Only for wind disturbances is the median overlap higher, with more than half of the S1DM polygons showing substantial coverage by IDS, indicating better agreement between the datasets for this disturbance type.

https://doi.org/10.5194/egusphere-2025-4880
Preprint. Discussion started: 12 November 2025

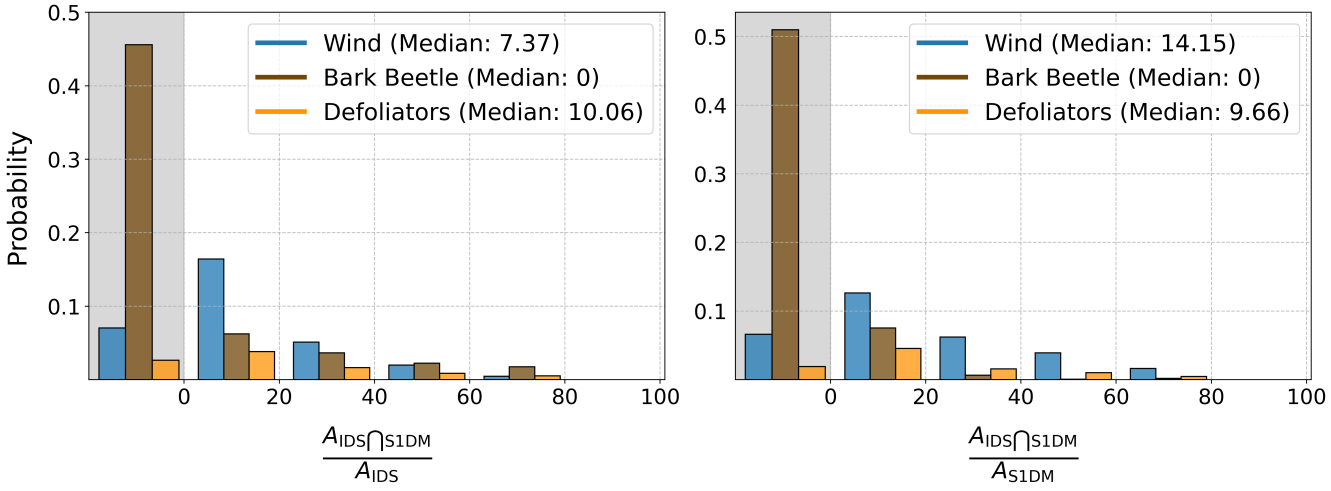

Figure 4. Probability of (a) IDS polygons being covered by S1DM, and (b) S1DM polygons overlapping with IDS, for each disturbance type. Disturbance types are color-coded as follows: Wind (blue), Bark Beetle (brown), and Defoliators (yellow). Median probabilities for each disturbance type are indicated in parentheses in the legend.

To explore whether overlap differences arise from variations in polygon sizes, spatial spread, or spatial offsets between IDS and S1DM events, we analyzed these three spatial properties (calculated in 3.3) for the disturbance events in IDS and S1DM, as shown in Figure 5 and Table 2.

Disturbance Type	Dataset	A_D 50% (km^2)	A_D 90% (km^2)	A_{CH} 50% (km^2)	A_{CH} 90% (km^2)	$\Delta_{Centroid}$ 50% (m)	$\Delta_{Centroid}$ 90% (m)
Wind	IDS	0.24	5.06	0.24	5.06	329.57	755.78
Wind	S1DM	0.34	5.03	2.15	11.31	-	-
Bark Beetle	IDS	0.0046	0.076	0.0046	0.076	297.85	537.27
Bark Beetle	S1DM	0.0043	0.074	0.25	1.35	-	-
Defoliator	IDS	0.49	3.68	0.49	3.68	273.58	950.02
Defoliator	S1DM	0.50	6.33	2.64	15.27	-	-

Table 2. Summary of disturbance area and centroid shift metrics for IDS and S1DM datasets. The table compares the median (50%) and 90_{th} percentile of detected disturbance areas (A_D) and convex hulls (A_{CH}), as well as the centroid shift ($\Delta_{Centroid}$) between the datasets.

Our findings reveal no notable differences in the individual size of disturbances across different types of events (Panel a)). We find that Wind disturbances tend to be the largest events, with 50% of events having a size of 0.43 km^2 or smaller (90%

https://doi.org/10.5194/egusphere-2025-4880
Preprint. Discussion started: 12 November 2025

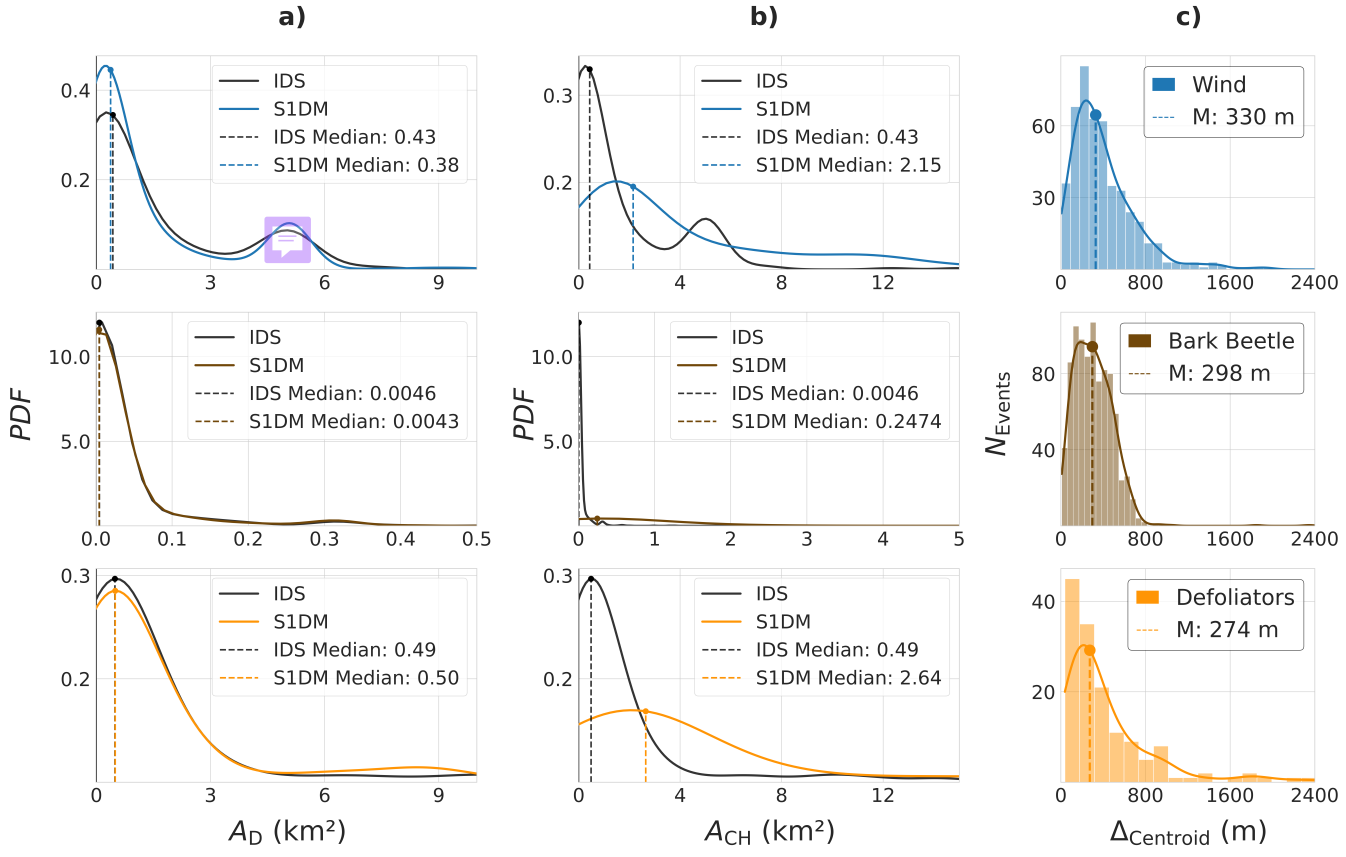

Figure 5. Comparison of disturbance size (in km^2) and spatial bias (in m) between the IDS and S1DM datasets. The figure consists of three vertical panels, each displaying the results for three disturbance types: Wind (top, blue), Bark Beetle (second, brown) and Defoliators (third, green). **a)** shows the probability density function (PDF) of disturbance patch areas for IDS (black lines) and S1DM (colored lines) across the four disturbance types. **b)** presents the PDF of the *convex-hull* (CH) areas, representing the spatial spread of the disturbance polygons, using the same color scheme for S1DM and IDS as in the left panel. **c)** displays histograms and corresponding PDFs of the spatial distance between IDS and S1DM centroids for each disturbance type.

smaller than 5.06 km^2), followed by Defoliators with a median area of 0.49 km^2 (90% below 3.68 km^2) and Bark Beetles with the smallest patches, with a median value of 0.0046 km^2 (90% smaller than 0.08 km^2).

We then compare the individual disturbance size estimated by S1DM with IDS. Overall, S1DM shows good agreement with IDS, with only minor differences across disturbance types. Bark Beetle disturbances show the closest match, as median values for IDS (0.0046 km^2) and S1DM (0.0043 km^2) are nearly identical, and 90% of events in both datasets are smaller than 0.08 km^2. ~~50% of S1DM Wind events being 0.1 km^2 and 90% being 0.03 km^2 smaller than IDS.~~ Unlike other disturbance types, Defoliator disturbances are slightly larger in S1DM compared to IDS. For Defoliators, ~~more than 50%~~ of S1DM events ~~are~~ 0.01 km^2 larger than ~~their~~ IDS counterparts~~,~~ and 90% of events ~~are~~ nearly twice as large in S1DM as in IDS.

https://doi.org/10.5194/egusphere-2025-4880
Preprint. Discussion started: 12 November 2025

Figure 5, panel b) illustrates the area of the convex hulls enclosing the IDS and S1DM polygons, which serves as an indicator of how spatially dispersed each disturbance event is. In the IDS dataset (without buffer), each event is represented by a single, compact polygon. In contrast, the corresponding S1DM event may consist of multiple scattered polygons (a multipolygon) encompassing all S1CD patches within the 500 m buffer applied during S1DM generation. This results in spatially fragmented event structures, as shown in Figure A1. Accordingly, panel b) demonstrates that S1DM events exhibit a substantially larger spatial extent than the corresponding IDS polygons across all disturbance types. These ratios, reflecting the relative spatial spread of S1DM to IDS, are also summarized and calculated form the values in Table 2. The median convex hull area of S1DM polygons is 5.3 times greater for Defoliators (0.49 (IDS) $\longrightarrow$ 2.64 (S1DM) km^2) and 8.5 times greater for Wind (0.24 $\longrightarrow$ 2.15 km^2) than for the respective IDS polygons. At the 90th percentile, these differences narrow, with the S1DM spread being 4.1 times larger for Defoliators (3.68 $\longrightarrow$ 15.27 km^2) and 2.2 times larger for Wind (5.06 $\longrightarrow$ 11.31 km^2). Bark beetle disturbances show the most pronounced increase, with the convex hull area more than 50 times larger for 50 % of events (0.0046 $\longrightarrow$ 0.25 km^2) and 17.8 times larger for 90 % of events (0.076 $\longrightarrow$ 1.35 km^2), although their overall affected area remains comparatively small, as discussed in panel a).

We further analyse the spatial bias between the centers of IDS and S1DM disturbance events (Figure 5 Panel c). Despite the pronounced differences in spatial extent and fragmentation, the centroids of corresponding events in both datasets remain closely aligned. Most S1DM centroids fall within 200–350 m of their respective IDS polygon centroids, indicating a strong spatial correspondence between mapped disturbance locations. Even at the 90th percentile, centroid distances remain below 1 km for the majority of events, suggesting that while S1DM polygons are more spatially dispersed, their overall positioning relative to IDS remains consistent.

We analyzed the temporal agreement between corresponding events in IDS and S1DM (Figure 6). We assess the temporal agreement between the datasets by identifying, for each IDS event, the corresponding S1DM detection year that is temporally closest. This allows us to quantify how many of the S1DM-detected disturbances correctly coincide in time with those reported by IDS. Overall, S1DM captures the timing of most disturbance events accurately, as reflected by the high number of events detected at a temporal lag of zero (Lag=0) across all disturbance types. Specifically, for Wind disturbances, 443 out of 469 S1DM events (94.5 %) occur in the same year as the corresponding IDS events, indicating excellent temporal agreement. For Defoliators, 92 out of 144 S1DM detections (63.9 %) coincide with the IDS year (Lag=0), demonstrating moderate agreement but a clear temporal correspondence between the two datasets. Both Wind and Defoliator events exhibit only limited temporal mismatch, with detections outside the IDS year (Lag=$\pm$1 or $\pm$2) accounting for less than 3 % of Wind and 29 % of Defoliator events, respectively. This indicates that, for these disturbance types, S1DM tends to identify a disturbance within the correct year. In contrast, Bark beetle disturbances display a broader temporal distribution. While a majority of events — 359 out of 899 (39.9 %) — are detected by S1DM in the same year as IDS (Lag=0), a substantial number fall within the $\pm$ 1 $\pm$1-year window around the IDS detection year, with 140 events (15.6 %) detected one year earlier and 157 events (17.5 %) one year later. Notably, 212 events (23.6 %) are detected by S1DM approximately two years earlier than IDS — representing the second-largest peak after Lag=0. This pattern suggests that bark beetle disturbances may be identified earlier in radar-based data, potentially capturing the onset of canopy-structure changes before visible defoliation is recorded in IDS.

https://doi.org/10.5194/egusphere-2025-4880
Preprint. Discussion started: 12 November 2025

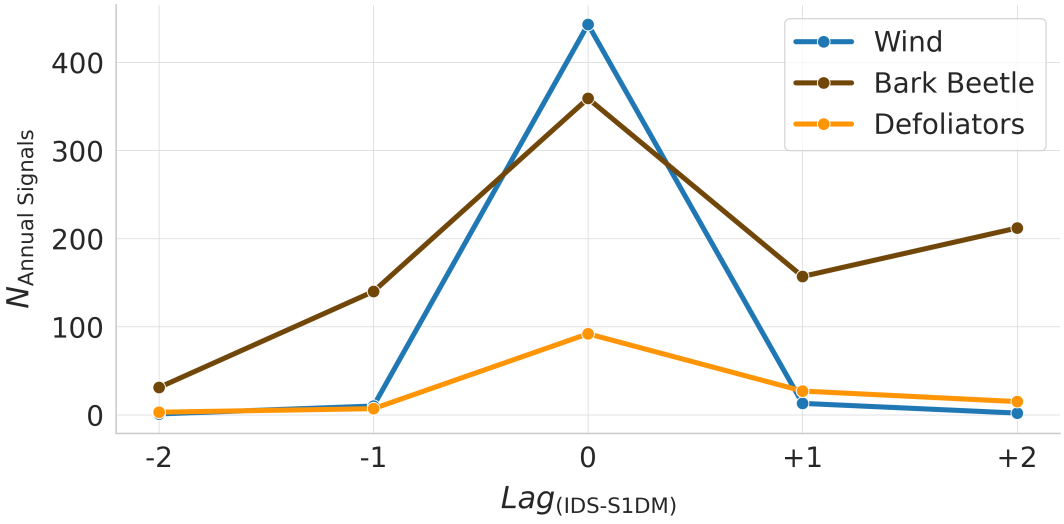

Figure 6. Temporal relationship between disturbance detection by S1CD and IDS. The x-axis represents the temporal yearly agreement with IDS - S1CD. Negative values indicate that IDS recorded the disturbance before S1CD detected it. The y-axis shows the count of events corresponding to each year's lag, with different disturbance types represented by distinct colored lines. We focuses on the single S1DM timestamp closest to the IDS year for each event. We calculate the temporal lag by subtracting the S1DM detection year from the IDS year. Negative values indicate that S1DM detection occurred after IDS, while positive values indicate earlier radar detection.

The temporal agreement of the S1CD signal should, however, be interpreted cautiously, as we find prolonged signals within the ±2-year time window used for the trend-break detection A2. For example, due to the detection algorithm, it is possible for a Wind event to be detected over multiple consecutive years, although such events are in fact abrupt. Furthermore, temporally continuous signals may reflect other changes, such as clear-cutting or restoration activities post-disturbance. This issue will be further explored in Section 5.

4.2 Assessment of spatial patterns in disturbed patches

Since both the S1DM and the IDS datasets exhibit spatial as well as temporal uncertainties (see Sections 2.2), we conducted an assessment of their temporal and spatial accuracy relative to a set of 15 manually labelled events per disturbance type based on PlanetScope images (see Methods). Figure 7 illustrates three representative disturbance events for Wind (first row), Bark Beetle (second row), and Defoliators (third row), where the polygons of our manual labels, IDS and S1DM are overlayed on the RGB composite of the first image showing a disturbance event in that location. For these examples, S1DM appears to capture the spatial extent of disturbances more accurately than IDS. For example, for Defoliator and Bark Beetle events IDS identifies a smaller area than the RGB composite indicates, whereas for Wind disturbances, both IDS and S1DM appear to identify disturbed areas that are not evident in the RGB composite (and thus our manually defined polygon). Overall, the S1DM polygons also appears to show more patchy and irregular spatial outlines compared to both manual and IDS polygons.

https://doi.org/10.5194/egusphere-2025-4880
Preprint. Discussion started: 12 November 2025

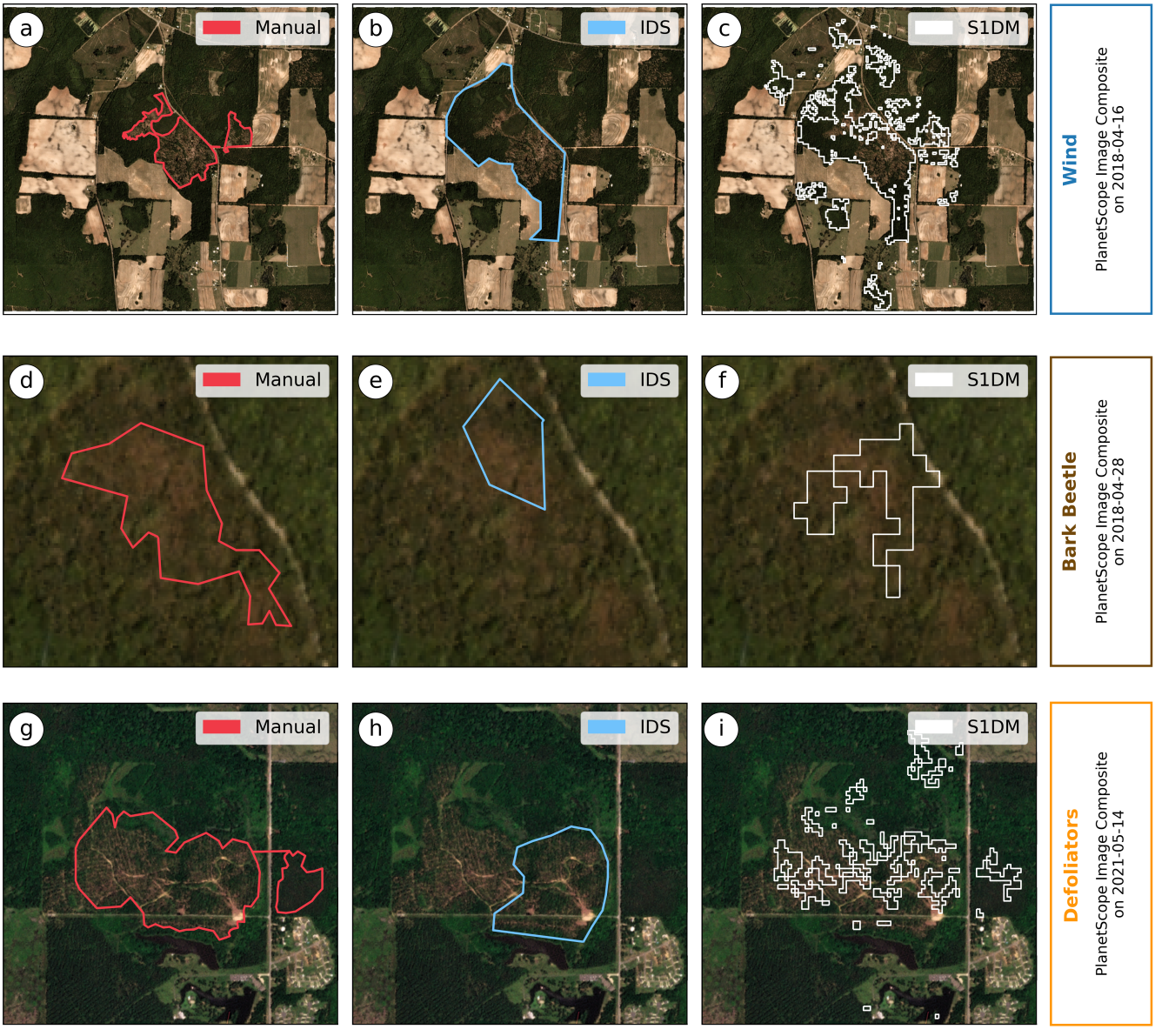

Figure 7. Spatial analysis of forest disturbance datasets using PlanetScope (3m) imagery, illustrating different labeling approaches: manual delineation (red), IDS (blue), and S1DM (white). Images are arranged row-wise by disturbance type (Wind, Defoliators, Bark Beetle) and displayed over the corresponding PlanetScope scene composites. In the first column (panels a, d, g), the manual polygons delineated using PlanetScope imagery are shown. The second column (panels b, e, h) shows the corresponding IDS polygons in light blue, while the third column (panels c, f, i) presents the S1DM polygons in white.

https://doi.org/10.5194/egusphere-2025-4880
Preprint. Discussion started: 12 November 2025

In Figure 8, we quantify the spatial agreement of IDS and S1DM polygons with the 3×15 manually labelled polygons from PlanetScope imagery, using both percentage overlap and the Jaccard similarity index (see Methods 3.5). S1DM polygons show substantially higher agreement with manual labels than IDS for Wind and Bark Beetle disturbances, with median values (see Tab. A4) of Jaccard Similarity (panel (a)) of 0.157 and 0.076 for Wind and Bark Beetle events detected by S1DM, respectively, compared to 0.092 and 0.007 for IDS. For the spatial overlap, S1DM estimates a median value of 44.3%, 20.1%, and 22.2% for Wind, Bark Beetle and Defoliators, compared to 12.3%, 0.7%, and 22.7% for IDS.

One-sided t-tests indicate that the improvement in the spatial agreement is significant for both Wind and Bark Beetle with both metrics, although for Wind only at 90% significance for the Jaccard Similarity. No statistically significant improvement is observed for Defoliator disturbances according to the t-test. It is worth noting that overall, the Jaccard similarity remains generally low, consistently below 0.4, while the percentage overlap ranges between 0% and 60%. This might be due both to uncertainties in S1DM and IDS, but also due to the visual labelling approach that relies on RGB signal.

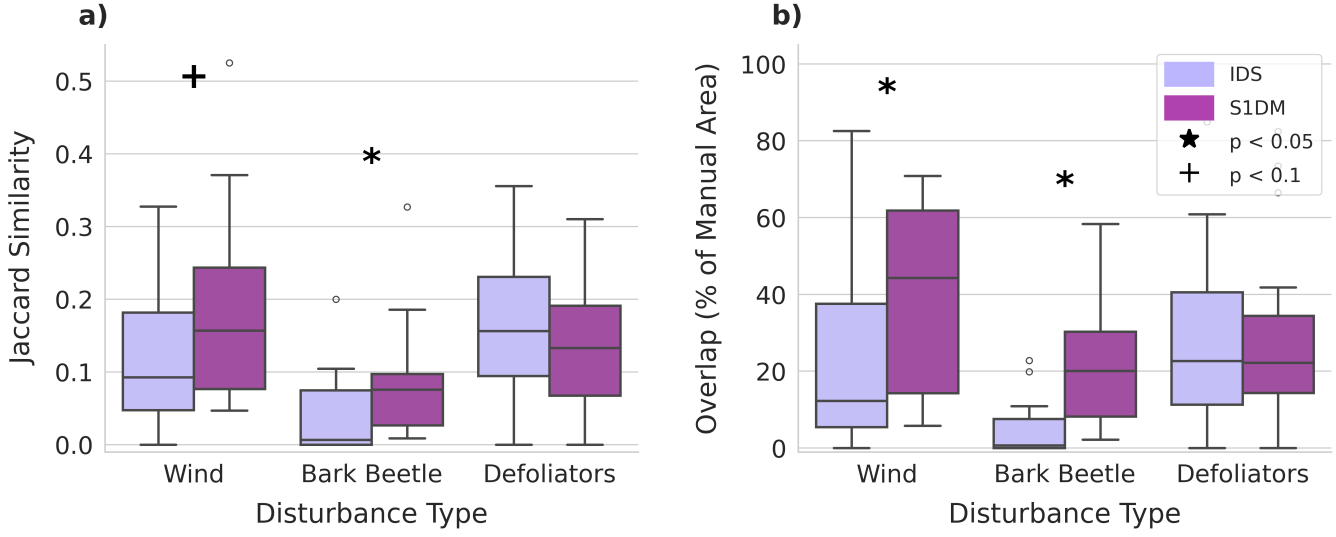

Figure 8. Comparison of agreement between IDS and S1DM disturbance maps with manually delineated reference polygons. Panel (a) shows the Jaccard similarity, and panel (b) shows area overlap (in percentage), both displayed as box plots. Statistical significance from a one-sided t-test is indicated by a black star for $p < 0.05$ and a black cross for $p < 0.1$.

https://doi.org/10.5194/egusphere-2025-4880
Preprint. Discussion started: 12 November 2025

5 Discussion

This paper aimed to develop a new disturbance dataset based on inventory data and refined by combining with radar information from satellite. To achieve this, we leveraged the strengths of the IDS: its extended temporal coverage, broad spatial extent, and detailed information about forest disturbance agents. We focused on a subset of disturbance events, specifically the most severe events, while excluding extremely large disturbances that are less reliably captured in IDS. By complementing the inventory data from IDS with radar data from Sentinel-1, which offered continuous, high-resolution spatial and temporal information on structural changes in forests, we aimed to better characterize the location and spatial patterns of disturbance events, as well as the corresponding disturbance timing. Such precise spatial and temporal information is crucial for using disturbance datasets in other applications, such as training increasingly popular yet data-intensive deep-learning models for forest disturbance classification.

5.1 Capabilities and Limitations of Sentinel-1 Change Detection to Improve Forest Disturbance Monitoring

Here, we produced new forest disturbance maps for the southeastern USA covering the period 2016-2021 based on the Sentinel-1 radar backscatter trend detection algorithm by Cremer et al. (2020), S1CD. This algorithm enhanced forest disturbance monitoring by leveraging Sentinel-1's frequent, consistent, and cloud-penetrating radar data to detect significant structural changes in forests. S1CD effectively identified disturbances associated with structural damage, such as bark beetle infestations and storms. As shown in Fig. 3, S1CD successfully detected over 75% of IDS-recorded wind and bark beetle disturbances in the study region and selected period. However, detection rates dropped significantly for more subtle disturbances, such as those caused by defoliators, where only 67% of disturbances reported by IDS were identified by S1CD.

This limitation is consistent with known challenges in remote sensing of forest disturbances, where gradual or low-intensity disturbances often remain undetected (McDowell et al., 2015). In this case, the low sensitivity of S1CD to subtle and slow-onset disturbances might stem from the change detection threshold, set at -1.28 (1/yr) by European Commission. Joint Research Centre. (2023). Since the method was optimized for detecting abrupt and permanent structural changes, disturbances that unfold gradually or cause only minor canopy loss are likely to have remained undetected. Although lowering the threshold could improve the sensitivity to these subtle disturbances, it would risk increasing noise, leading to more false positives and reducing the detection reliability. Thus, while the Sentinel-1 Change Detection method applied here was highly effective in capturing severe disturbances such as wind-throw and bark beetle outbreaks, its limitations in detecting milder, gradual, or recovering disturbances must be acknowledged.

Additionally, in our IDS pre-processing, we excluded all temporally compound events to retrieve a clear disturbance signal for each disturbance agent. However, by excluding such events, we introduced bias into the dataset, so that our hybrid S1–IDS dataset (S1DM) should not be considered for exhaustive characterization of disturbance occurrence in the study region. While not representative of all disturbance events, the dataset provides a set of "noise-free" disturbance events for each of the four agents considered, which should allow for better training of unsupervised classification models. Below, we discuss the improvements introduced by our hybrid dataset.

https://doi.org/10.5194/egusphere-2025-4880
Preprint. Discussion started: 12 November 2025

5.1.1 (1) Location and delineation of disturbance patches

Previous studies (Backsen and Howell, 2013; McConnell, 2000) noted the challenges in accurately mapping disturbances using aerial surveys, mainly due to the high speeds at which these surveys are conducted. Aircraft speeds of 144–200 km/h ~~(100 mph)~~ and altitudes ranging from 305 to 762 meters above the canopy make the accurate delineation of disturbance patches difficult (Coleman et al., 2018). To address this limitation, we applied a 500-meter buffer around disturbance locations, which we had determined in the Methods 3.4 as an optimal trade-off between retaining relevant events and minimizing noise. The results, shown in Figure 5c) and Table 2, indicated that 50% of S1DM disturbance centers fall within 200–400 meters of IDS centroids, with most events within 950 meters. This suggests that the centers of disturbance patches from both datasets are generally well-aligned within the inherent uncertainty of aerial detection surveys.

Our results align with studies showing limitations to the accuracy of aerial surveys, particularly their tendency to overestimate disturbance areas and include healthy, unaffected trees (Hall et al., 2016; Kautz, 2014). We found that the total disturbed area was generally consistent between the two datasets. For 50% of disturbance events, the size difference was less than 0.2 km^2 (Figure 5a). However, spatial discrepancies remain important. Specifically, Fig. 4 shows that, on average, less than 10% of the area of IDS disturbance polygons overlaps with S1DM polygons. Similarly, less than 15% of the area of an S1DM polygon is covered by the corresponding IDS polygon, highlighting substantial differences in the spatial distribution of disturbances between the two datasets.

The limited spatial overlap between IDS and S1DM disturbance patches arises from several factors. IDS polygons tend to be large, single polygons, whereas S1DM polygons are often multipolygons, with gaps and holes, resulting in only partial spatial correspondence (Figure 7). In addition, IDS patches, particularly for Wind and Defoliator events, often exhibit artificial geometric shapes such as rectangles or squares. These shapes are atypical for natural disturbances and may include healthy, unaffected trees within the polygons (Hall et al., 2016; Kautz et al., 2017; Kautz, 2014). In contrast, S1DM identifies smaller, more irregular patches that better reflect the natural variation of disturbance processes.

S1DM disturbances are frequently distributed around IDS polygons, forming multiple discrete patches that aggregate to a similar total area but with minimal spatial overlap (Figures 7b,c and e,f). Slight misalignments or offsets between IDS and S1DM patches further reduce overlap, even when the disturbance sizes are similar (Figures 7b,d). This pattern is supported by the analyses in Figure 5 and Table 2, which indicate that S1DM disturbances often cover a wider area compared to IDS.

However, Figure 7 also illustrates that S1DM can sometimes miss patches entirely, as exemplified in panel i, while in other cases it aligns well with IDS patches (panels b–c). This is primarily due to the threshold applied during the Sentinel-1 change detection, where some polygons may not meet the disturbance criteria or fall below the threshold for detection.

Our quantitative analysis (Figure 8) further supports these observations. Randomly sampled elements show that wind and bark beetle events are captured more consistently by S1DM compared to IDS and align better with manual assessments. Only defoliator events show no significant improvement relative to IDS. This highlights both the strengths of S1DM in representing disturbance processes more realistically and its limitations, where the detection threshold can lead to missed events.

https://doi.org/10.5194/egusphere-2025-4880
Preprint. Discussion started: 12 November 2025

Importantly, our analysis underscores that IDS and S1DM can complement each other. While IDS offers a broad, initial assessment, S1DM excels at delineating the disturbance patches in more detail and detecting disturbed patches that may be missed due to spatial misalignments or the limitations of IDS in capturing the full extent of disturbances. This advantage of S1DM is particularly evident for wind and bark beetle disturbances, where it provides clearer and more realistic patch delineations. However, for defoliator events, S1DM does not show the same improvement over IDS. Therefore, we are confident that our hybrid dataset, S1DM, can provide an improved reference dataset for disturbed areas, facilitating the development of remote-sensing-based classification models.

5.1.2 (2) Timing of disturbances

Accurately assigning the timing of a given disturbance event is generally challenging. Both IDS and S1DM are subject to inherent temporal uncertainties due to their acquisition methods and characteristics. For IDS, temporal uncertainties stem from the nature of aerial surveys. Flights do not always happen at optimal times due to weather, logistics, or survey schedules, leading to disturbances being recorded late or at suboptimal times (McConnell, 2000). This issue is particularly pronounced for biotic disturbances, such as defoliators and bark beetles. Defoliators must be mapped while actively feeding; if surveyors fly too early or too late, the disturbance may be underestimated or missed entirely. Similarly, bark beetle outbreaks often go undetected until tree mortality becomes widespread, creating a delay between the initial attack and recorded detection (Kautz, 2014). Recent work by (Eifler et al., 2024) estimated an average delay of one year between IDS and plot-scale forest inventory information.

Given that IDS already has an average temporal misalignment of over a year, we applied a two-year buffer when comparing IDS and S1DM to ensure a more realistic temporal intersection. Figure 6 illustrates the challenge of precisely pinpointing the timing of the disturbance. The left panel shows that S1DM detected change signals for all disturbance types in the years surrounding the IDS disturbance year. Still, the right panel focuses on the S1DM signal that temporally aligns most closely with the IDS disturbance year for each event.

For those events in which S1DM detects a disturbance earlier than IDS, the event likely began the year before it was detected by aerial surveys, indicating potentially a better ability of S1CD for early detection of the onset of disturbance. However, we cannot exclude artefacts resulting from S1DM's built-in ± 0.5-year temporal buffer for trend detection that can cause some disturbances to be attributed to the wrong year. The uncertainty due to the temporal buffer in S1DM could also explain the later detection compared to IDS. However, it could also have a physical reason, especially for events in which human-driven post-disturbance actions, such as salvage logging or clear-cutting, result in more pronounced changes in forest structure, which are better captured by the trend detection algorithm.

Biotic disturbances further complicate this, as insect outbreaks can persist for multiple years. Recurring defoliation attacks, for instance, can result in consecutive-year detections that do not necessarily indicate misattribution but rather repeated disturbances. While we excluded disturbed patches that temporally and spatially overlapped in IDS, we cannot exclude the detection of such compound events in S1DM in their close vicinity. Similarly, changes in signals after post-disturbance years in fire and wind events may reflect salvage logging rather than ongoing disturbance.

https://doi.org/10.5194/egusphere-2025-4880
Preprint. Discussion started: 12 November 2025

Disturbance events occur within a complex ecosystem influenced by multiple factors. Gradual mortality, delayed detection, and human-driven post-disturbance actions (e.g., salvage logging or clear-cutting) further complicate the precise determination of disturbance timing. Because we cannot fully disentangle these complexities, we considered the IDS survey year as the reference for further analysis. Figure 6 shows that for most disturbance events, at least part of the detected disturbance was assigned the same year as the IDS survey. However, a notable exception is the number of bark beetle events detected two years before IDS.

5.2 Alternative to Manual Labeling Practices

In addition to providing an improved hybrid forest disturbance reference dataset for disturbance agent classification, our approach aimed to move beyond the traditional, labor-intensive method of manual labeling. The Sentinel-1 Change Detection (S1CD) algorithm enables analysts to bypass the time-consuming task of manually refining disturbance locations, outlines, and timing by using high-resolution radar-based information on forest structure and change. By employing the trend break detection by European Commission. Joint Research Centre. (2023), we successfully automated much of the re-labeling process, creating an efficient and scalable system that requires a smaller contribution of expert knowledge. This not only reduces the need for manual inspection but also offers a viable alternative to manual labor, minimizing reliance on private, sometimes exploitative labor platforms located in developing countries, as is often the case for deep learning label generation (Aloisi, 2016; Hawkins and Mittelstadt, 2023).

Our semi-automatic labeling method, was initially developed to tackle specific challenges related to reference dataset quality (see 1). A key advantage of our semi-automated labeling method is its adaptability to different regions, as long as some form of inventory-based disturbance data, e.g. the Canadian Forest Service's National Forestry Database (NFD), the Database of Forest Disturbances in Europe (Patacca et al., 2021, DFDE), the Dataset of Wind Disturbances in European Forests (Forzieri et al., 2020, FORWIND), or the Database of European Forest Insect and Disease Disturbances (Forzieri et al., 2020, DEFID2), is available. Sentinel-1 data, available globally since 2014, provides a consistent and uninterrupted record of forest dynamics. Unlike optical datasets, such as Sentinel-2, which are susceptible to cloud cover and atmospheric interference, Sentinel-1's radar data offer reliable time series analysis across diverse climatic conditions. This robustness makes it particularly valuable for monitoring large-scale and long-term disturbances.

However, Sentinel-1 data is affected by terrain-induced distortions in mountainous regions, which can reduce classification accuracy (Small, 2011; Imperatore, 2021). Users should exercise caution when applying this method in areas with significant elevation changes, as radar signal distortions can impact data reliability. Despite this limitation, our approach remains broadly applicable, especially in flat or gently sloping landscapes with more stable radar performance.

6 Conclusion

Global-scale, consistent data on forest disturbances caused by natural hazards, such as wind, insect outbreaks, pathogens, and diseases, is critically lacking, as existing data remains sparse and biased across different regions. While large-scale forest

https://doi.org/10.5194/egusphere-2025-4880
Preprint. Discussion started: 12 November 2025

disturbance inventories such as IDS provide valuable insights, they are often derived from aerial detection surveys, which suffer from inherent spatial and temporal uncertainties. Rapid decision-making during high-speed flights, coupled with weather and logistical constraints, can lead to inaccuracies in disturbance location, outline, and timing. Variability in biotic disturbances further exacerbates these issues.

To overcome these limitations, we developed an alternative method that refines existing disturbance inventories by integrating IDS with a change detection algorithm based on Sentinel-1 radar data (S1CD). This approach leverages the strengths of both datasets: IDS provides visual, inventory-based information, while S1DM captures structural changes via radar.

In our analysis, we aimed to improve three specific issues: locational uncertainty, outline accuracy, and temporal uncertainty in the dataset. Although S1CD performed less well with subtle disturbances (e.g., defoliators), it demonstrated good skill in capturing fast-onset, structurally significant events, such as wind damage and bark beetle outbreaks. Spatially, the locations of disturbance centers were generally within 200–950 meters of each other. Although the overall disturbed area remained similar between datasets, the S1DM dataset identifies more realistic disturbance patterns, with Wind and Bark Beetle showing significantly better overlap with the manual ground truth.

Our hybrid dataset thus offers an improved reference dataset on forest disturbances that can be used to enhance the accuracy of disturbance mapping and facilitate the analysis of different disturbance types, representing an advance in methods for mapping disturbances. The methodology supports the development of fully automatic forest disturbance classification methods. Despite these advances, uncertainties remain regarding the precise timing and duration of disturbances. Future work could explore other techniques, such as reinforcement learning techniques, to combine IDS, S1DM, and Sentinel-2 data and further enhance forest disturbance classification, particularly for cases where neither dataset fully captures the disturbance signal. Finally, our approach provides a scalable and less labour-intensive alternative to manual labeling, and is transferable to other regions and reference datasets.

https://doi.org/10.5194/egusphere-2025-4880
Preprint. Discussion started: 12 November 2025

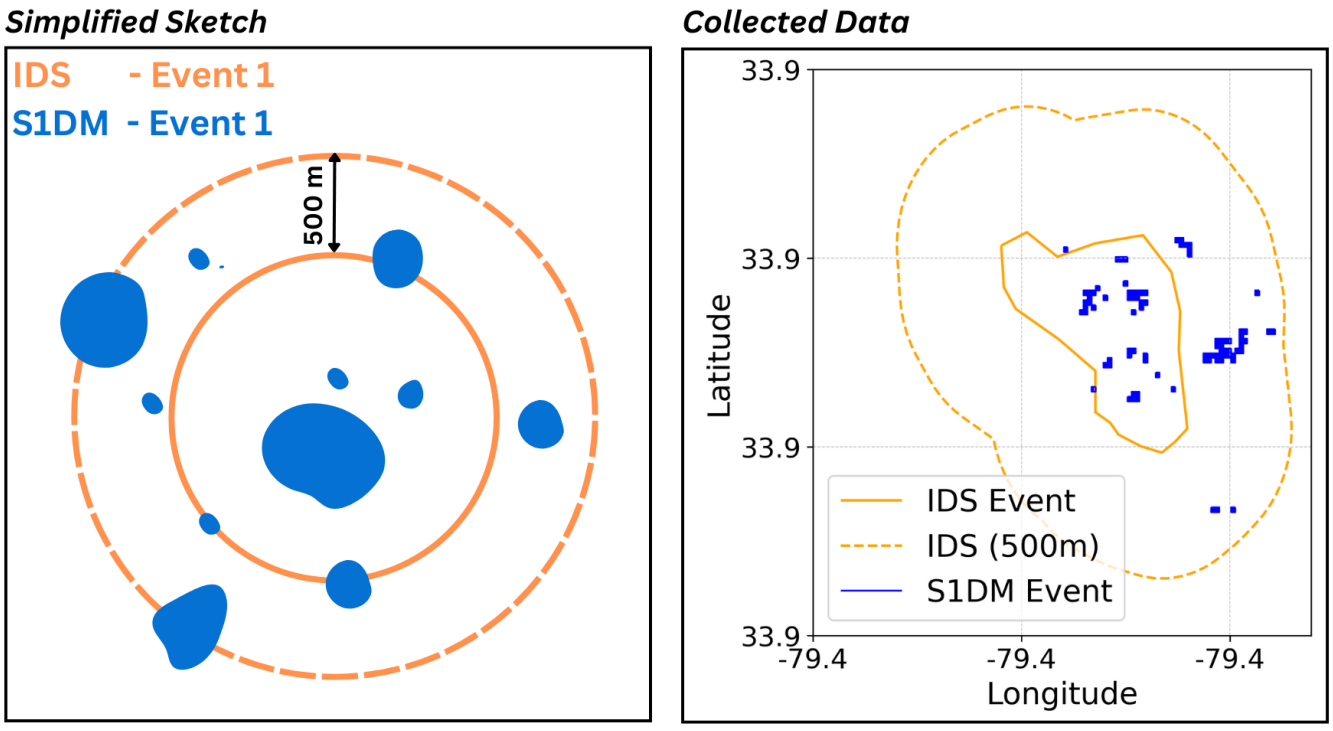

Figure A1. Schematic (left) and data-driven (right) representations of the intersection between IDS and S1CD. On the left, a conceptual diagram illustrates how each S1CD polygon intersecting with an IDS event's buffered (500m) boundary is combined into a multi-polygon, effectively merging multiple S1CD polygons associated with a single IDS event. The right panel illustrates this process applied to real data, where intersecting S1CD polygons are grouped and treated as a single unified event, similar to the treatment of IDS polygons.

https://doi.org/10.5194/egusphere-2025-4880
Preprint. Discussion started: 12 November 2025

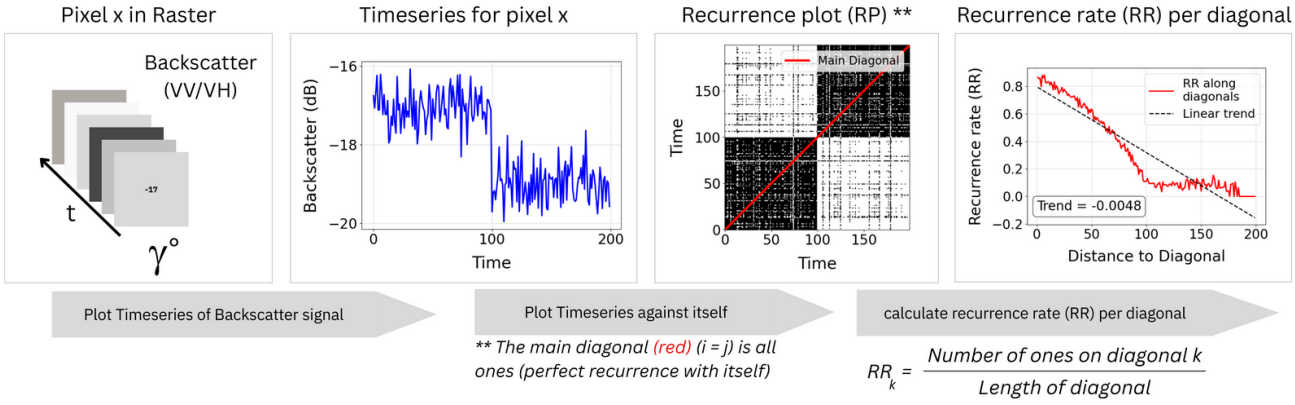

Figure A2. Schematic representation of recurrence analysis for a Gamma backscatter pixel. (a) Singular Pixel of one Sentinel-1 Raster Tile (b) Time series of the pixel showing a sudden change ("break") in backscatter values. (c) Recurrence plot (RP) highlighting times when the signal revisits similar states; the main diagonal is shown in red. (d) Recurrence rate (RR_i) computed along off-diagonals of the RP, with a linear trend (dashed line) indicating the rate of drift in the system. The slope of the trend quantifies whether the process is stationary or drifting over time.

Table A1. Comprehensive list of tree species in the study area

Region	**Dominant Species**
Entire Region	White Oak (*Quercus alba*), Red Oak (*Quercus rubra*), Hickory (*Carya spp.*), Loblolly Pine (*Pinus taeda*), Slash Pine (*Pinus elliottii*)
Southern Region	Sand Pine (*Pinus clausa*), Baldcypress (*Taxodium distichum*), Water Tupelo (*Nyssa aquatica*), Sugarberry (*Celtis laevigata*), Hackberry (*Celtis occidentalis*), Elm (*Ulmus spp.*), Green Ash (*Fraxinus pennsylvanica*), Virginia Pine (*Pinus virginiana*), Sweetgum (*Liquidambar styraciflua*), Yellow-poplar (*Liriodendron tulipifera*)
Appalachian Region	Chestnut Oak (*Quercus montana*), Eastern White Pine (*Pinus strobus*), Sugar Maple (*Acer saccharum*), Beech (*Fagus grandifolia*), Yellow Birch (*Betula alleghaniensis*), Yellow-poplar (*Liriodendron tulipifera*), White Oak (*Quercus alba*), Northern Red Oak (*Quercus rubra*), Virginia Pine (*Pinus virginiana*), Southern Red Oak (*Quercus falcata*), various Mixed Upland Hardwoods

Equi7 NA Sentinel-1 Change Detection Grid Cells					
E093 N033T3	E099 N033T3	E084 N030T3	E087 N030T3	E090 N030T3	E093 N030T3
E099 N030T3	E084 N027T3	E087 N027T3	E090 N027T3	E093 N027T3	E096 N027T3
E084 N024T3	E087 N024T3	E090 N024T3	E093 N024T3	E096 N024T3	

Table A2. Equi7 Sentinel-1 Change Detection Grid Cells used over the region in North America, downloaded from Sentinel-1

https://doi.org/10.5194/egusphere-2025-4880
Preprint. Discussion started: 12 November 2025

Column Name	Description	Example
ID_E	Unique identifier for the event in the IDS dataset	43132
DCA_ID	Disturbance category identifier from IDS	wind
SURVEY_Y	Year the disturbance was recorded in IDS	2018
REGION_ID	Identifier for the geographical region in IDS reference to unique ID_E	8
DA_C_USDA	IDS classification of the disturbance type	16
ID_O	Identifier for overlapping events across datasets; references the ID_E of intersecting event	5678
O_Year	Year of overlapping event	2019
O_DCA_ID	Overlapping disturbance category ID	defoliators
O_Y_diff	Temporal difference (in years) between this ebevnt overlapping records	1
IDX_D	Index for tracking disturbance events	8_wind_2020_21436
area_km2	Area of the disturbance event in square kilometers	0.415069
geometry	Polygon geometry representing the spatial extent of the disturbance	POLYGON(...)
S1_YEAR	Year the disturbance was detected via radar satellite (S1CD dataset)	2019
S1_TILE	Identifier for the radar satellite tile	E090N030T3
S1CD_INDEX	Index for disturbance events detected by the S1CD dataset	11222

Table A3. Key columns in the S1DM geodataframe, documenting attributes of the disturbance events recorded by IDS and detected via the S1CD radar satellite.

Table A4. Median Jaccard similarity and area overlap (%) for IDS and S1DM polygons compared to manually labelled references.

Disturbance	Jaccard		Overlap (%)	
	IDS	S1DM	IDS	S1DM
Wind	0.092	0.157	12.3	44.3
Bark Beetle	0.007	0.076	0.7	20.1
Defoliators	0.156	0.133	22.7	22.2

https://doi.org/10.5194/egusphere-2025-4880
Preprint. Discussion started: 12 November 2025

Code availability. The code will be made publicly available upon publication.

Data availability. Insect and Disease Survey data by the U.S. Department of Agriculture can be downloaded at https://www.fs.usda.gov/science-technology/data-tools-products/fhp-mapping-reporting/detection-surveys; Tree Canopy Cover data from the U.S. Forest Service's Geospatial Technology and Applications Center is available at https://data.fs.usda.gov/geodata/rastergateway/treecanopycover/; S1CD and S1DM data will be made available upon publication.

Author contributions. AB and FM designed the study. LE performed IDS data preprocessing, FC conducted Sentinel-1 Change Detection, and FM managed overall data preprocessing (IDS, S1CD, and Sentinel-2) and analysis, with scientific and technical input from AB, GCV, PB and LE. FM wrote the first draft of the paper. All authors contributed to the final manuscript.

Competing interests. The authors declare that they have no conflicts of interest.

Acknowledgements. FM and AB acknowledge funding by the European Union (ERC StG, ForExD, grant agreement No. 101039567). GCV thanks funding from the European Research Council (ERC) under the ERC Synergy Grant USMILE (grant agreement 855187) and the H2020 project XAIDA (grant agreement 101003469). This work uses Copernicus Sentinel data 2016-2022. The generation of the S1CD data was supported by the ESA Network of Resources Initiative and the Copernicus – eoSC AnaLytics Engine (C-SCALE) project, which received funding from the European Union's Horizon 2020 research and innovation program under grant agreement No. 101017529. The views expressed are purely those of the writers and may not in any circumstances be regarded as stating an official position of the European Commission.

https://doi.org/10.5194/egusphere-2025-4880
Preprint. Discussion started: 12 November 2025

References

Aloisi, A.: Commoditized Workers. Case Study Research on Labour Law Issues Arising from a Set of 'On-Demand/Gig Economy' Platforms, https://doi.org/10.2139/ssrn.2637485, 2016.

Altman, J., Fibich, P., Trotsiuk, V., and Altmanova, N.: Global pattern of forest disturbances and its shift under climate change, Science of The Total Environment, 915, 170 117, https://doi.org/10.1016/j.scitotenv.2024.170117, 2024.

Anderegg, W. R. L., Hicke, J. A., Fisher, R. A., Allen, C. D., Aukema, J., Bentz, B., Hood, S., Lichstein, J. W., Macalady, A. K., Mcdowell, N., Pan, Y., Raffa, K., Sala, A., Shaw, J. D., Stephenson, N. L., Tague, C., and Zeppel, M.: Research review Tree mortality from drought, insects, and their interactions in a changing climate, New Phytologist, 208, 674–683, https://doi.org/10.1111/nph.13477, 2015.

Andresini, G., Appice, A., and Malerba, D.: A Deep Semantic Segmentation Approach to Map Forest Tree Dieback in Sentinel-2 Data, IEEE Journal of Selected Topics in Applied Earth Observations and Remote Sensing, 17, 17 075–17 086, https://doi.org/10.1109/JSTARS.2024.3460981, 2024.

Backsen, J. C. and Howell, B.: Comparing Aerial Detection and Photo Interpretation for Conducting Forest Health Surveys, Western Journal of Applied Forestry, 28, 3–8, https://doi.org/10.5849/wjaf.12-010, 2013.

Bae, S., Müller, J., Förster, B., Hilmers, T., Hochrein, S., Jacobs, M., Leroy, B. M. L., Pretzsch, H., Weisser, W. W., and Mitesser, O.: Tracking the temporal dynamics of insect defoliation by high-resolution radar satellite data, Methods in Ecology and Evolution, 13, 121–132, https://doi.org/10.1111/2041-210X.13726, 2022.

Bauer-Marschallinger, B., Sabel, D., and Wagner, W.: Optimisation of global grids for high-resolution remote sensing data, Computers & Geosciences, 72, 84–93, https://doi.org/10.1016/j.cageo.2014.07.005, 2014.

Bauman, D., Fortunel, C., Delhaye, G., Malhi, Y., Cernusak, L. A., Bentley, L. P., Rifai, S. W., Aguirre-Gutiérrez, J., Menor, I. O., Phillips, O. L., McNellis, B. E., Bradford, M., Laurance, S. G. W., Hutchinson, M. F., Dempsey, R., Santos-Andrade, P. E., Ninantay-Rivera, H. R., Chambi Paucar, J. R., and McMahon, S. M.: Tropical tree mortality has increased with rising atmospheric water stress, Nature, 608, 528–533, https://doi.org/10.1038/s41586-022-04737-7, 2022.

Byrne, B., Liu, J., Bowman, K. W., Pascolini-Campbell, M., Chatterjee, A., Pandey, S., Miyazaki, K., van der Werf, G. R., Wunch, D., Wennberg, P. O., Roehl, C. M., and Sinha, S.: Carbon emissions from the 2023 Canadian wildfires, Nature, 633, 835–839, https://doi.org/10.1038/s41586-024-07878-z, 2024.

Bárta, V., Lukeš, P., and Homolová, L.: Early detection of bark beetle infestation in Norway spruce forests of Central Europe using Sentinel-2, International Journal of Applied Earth Observation and Geoinformation, 100, 102 335, https://doi.org/10.1016/j.jag.2021.102335, 2021.

Canadell, J. G., Meyer, C. P. M., Cook, G. D., Dowdy, A., Briggs, P. R., Knauer, J., Pepler, A., and Haverd, V.: Multi-decadal increase of forest burned area in Australia is linked to climate change, Nature Communications, 12, 6921, https://doi.org/10.1038/s41467-021-27225-4, 2021.

Candotti, A., De Giglio, M., Dubbini, M., and Tomelleri, E.: A Sentinel-2 Based Multi-Temporal Monitoring Framework for Wind and Bark Beetle Detection and Damage Mapping, Remote Sensing, 14, 6105, https://doi.org/10.3390/rs14236105, 2022.

Chuvieco, E., Lizundia-Loiola, J., Pettinari, M. L., Ramo, R., Padilla, M., Tansey, K., Mouillot, F., Laurent, P., Storm, T., Heil, A., and others: Generation and analysis of a new global burned area product based on MODIS 250 m reflectance bands and thermal anomalies, Earth System Science Data, 10, 2015–2031, publisher: Copernicus GmbH, 2018.

https://doi.org/10.5194/egusphere-2025-4880
Preprint. Discussion started: 12 November 2025

Coleman, T. W., Graves, A. D., Heath, Z., Flowers, R. W., Hanavan, R. P., Cluck, D. R., and Ryerson, D.: Accuracy of aerial detection surveys for mapping insect and disease disturbances in the United States, Forest Ecology and Management, 430, 321–336, https://doi.org/10.1016/j.foreco.2018.08.020, 2018.

Cremer, F., Urbazaev, M., Cortés, J., Truckenbrodt, J., Schmullius, C., and Thiel, C.: Potential of Recurrence Metrics from Sentinel-1 Time Series for Deforestation Mapping, IEEE Journal of Selected Topics in Applied Earth Observations and Remote Sensing, 13, 5233–5240, https://doi.org/10.1109/JSTARS.2020.3019333, 2020.

Curtis, P. G., Slay, C. M., Harris, N. L., Tyukavina, A., and Hansen, M. C.: Classifying drivers of global forest loss, Science, 361, 1108–1111, https://doi.org/10.1126/science.aau3445, 2018.

Dalponte, M., Sassi, R., Gianelle, D., Bruzzone, L., and Marinelli, D.: Exploring the Detection of Bark Beetle Attacks in Norway Spruce Forests in Sentinel-1 Image Time Series, https://doi.org/10.1109/IGARSS53475.2024.10641531, 2024.

Eifler, L., Müller, F., and Bastos, A.: Evaluating the consistency of forest disturbance datasets in continental USA, EGUsphere, pp. 1–36, https://doi.org/10.5194/egusphere-2024-3534, 2024.

Eklundh, L., Johansson, T., and Solberg, S.: Mapping insect defoliation in Scots pine with MODIS time-series data, Remote Sensing of Environment, 113, 1566–1573, https://doi.org/10.1016/j.rse.2009.03.008, 2009.

European Commission. Joint Research Centre.: Proceedings of the 2023 conference on Big Data from Space (BiDS'23): from foresight to impact : 6 9 November 2023, Austrian Center, Vienna., Publications Office, LU, https://data.europa.eu/doi/10.2760/46796, 2023.

European Environment Agency (EU body or agency): European climate risk assessment: executive summary, Publications Office of the European Union, https://data.europa.eu/doi/10.2800/204249, 2024.

FAO: Global Forest Resources Assessment 2020 (FRA2020), Tech. rep., Food and Agriculture Organization of the United Nations, Rome, https://doi.org/10.4060/ca9825en, 2020.

Forest Service U.S. Department of Agriculture: Detection Surveys, https://www.fs.usda.gov/science-technology/data-tools-products/fhp-mapping-reporting/detection-surveys, data downloaded: 12.03.2024, 2024.

Forzieri, G., Pecchi, M., Girardello, M., Mauri, A., Klaus, M., Nikolov, C., Rüetschi, M., Gardiner, B., Tomaštík, J., Small, D., Nistor, C., Jonikavicius, D., Spinoni, J., Feyen, L., Giannetti, F., Comino, R., Wolynski, A., Pirotti, F., Maistrelli, F., Savulescu, I., Wurpillot-Lucas, S., Karlsson, S., Zieba-Kulawik, K., Strejczek-Jazwinska, P., Mokroš, M., Franz, S., Krejci, L., Haidu, I., Nilsson, M., Wezyk, P., Catani, F., Chen, Y.-Y., Luyssaert, S., Chirici, G., Cescatti, A., and Beck, P. S. A.: A spatially explicit database of wind disturbances in European forests over the period 2000–2018, Earth System Science Data, 12, 257–276, https://doi.org/10.5194/essd-12-257-2020, 2020.

Forzieri, G., Girardello, M., Ceccherini, G., Spinoni, J., Feyen, L., Hartmann, H., Beck, P. S. A., Camps-Valls, G., Chirici, G., Mauri, A., and Cescatti, A.: Emergent vulnerability to climate-driven disturbances in European forests, Nature Communications, 12, 1081, https://doi.org/10.1038/s41467-021-21399-7, number: 1 Publisher: Nature Publishing Group, 2021.

Forzieri, G., Dutrieux, L. P., Elia, A., Eckhardt, B., Caudullo, G., Álvarez Taboada, F., Andriolo, A., Bălăcenoiu, F., Bastos, A., Buzatu, A., Castedo Dorado, F., Dobrovolný, L., Duduman, M.-L., Fernandez-Carrillo, A., Cescatti, A., A Beck, P. S., Giovanni Forzieri, C., and Commission, E.: The Database of European Forest Insect and Disease Disturbances: DEFID2, Glob Change Biol, 00, 30, https://doi.org/10.1111/gcb.16912, 2023.

Gibson, R., Danaher, T., Hehir, W., and Collins, L.: A remote sensing approach to mapping fire severity in south-eastern Australia using sentinel 2 and random forest, Remote Sensing of Environment, 240, 111 702, https://doi.org/10.1016/j.rse.2020.111702, 2020.

Graziosi, I., Tembo, M., Kuate, J., and Muchugi, A.: Pests and diseases of trees in Africa: A growing continental emergency, PLANTS, PEOPLE, PLANET, 2, 14–28, https://doi.org/10.1002/ppp3.31, 2020.

https://doi.org/10.5194/egusphere-2025-4880
Preprint. Discussion started: 12 November 2025

Hall, R., Castilla, G., White, J., Cooke, B., and Skakun, R.: Remote sensing of forest pest damage: a review and lessons learned from a Canadian perspective, The Canadian Entomologist, 148, S296–S356, https://doi.org/10.4039/tce.2016.11, 2016.

Hammond, W. M., H., Williams, A. P., Abatzoglou, J. T., Adams, H. D., Klein, T., López Rodríguez, R., Sáenz-Romero, C., Hartmann, H., Breshears, D. D., and Allen, C. D.: Global field observations of tree die-off reveal hotter-drought fingerprint for Earth's forests, Nature Communications, data downloaded: 28.04.2022, 2022.

Hansen, M. C. and Loveland, T. R.: A review of large area monitoring of land cover change using Landsat data, Remote Sensing of Environment, 122, 66–74, https://doi.org/10.1016/j.rse.2011.08.024, 2012.

Hansen, M. C., Potapov, P. V., Moore, R., Hancher, M., Turubanova, S. A., Tyukavina, A., Thau, D., Stehman, S. V., Goetz, S. J., Loveland, T. R., Kommareddy, A., Egorov, A., Chini, L., Justice, C. O., and Townshend, J. R.: High-resolution global maps of 21st-century forest cover change, Science, 342, 850–853, https://doi.org/10.1126/SCIENCE.1244693, data downloaded: 09.08.2022, 2013.

Harris, N. L., Brown, S., Hagen, S. C., Saatchi, S. S., Petrova, S., Salas, W., Hansen, M. C., Potapov, P. V., and Lotsch, A.: Baseline Map of Carbon Emissions from Deforestation in Tropical Regions, Science, 336, 1573–1576, https://doi.org/10.1126/science.1217962, publisher: American Association for the Advancement of Science, 2012.

Harris, N. L., Hagen, S. C., Saatchi, S. S., Pearson, T. R. H., Woodall, C. W., Domke, G. M., Braswell, B. H., Walters, B. F., Brown, S., Salas, W., Fore, A., and Yu, Y.: Attribution of net carbon change by disturbance type across forest lands of the conterminous United States, Carbon Balance and Management, 11, 24, https://doi.org/10.1186/s13021-016-0066-5, 2016.

Hartmann, H., Bastos, A., Das, A. J., Esquivel-Muelbert, A., Hammond, W. M., Martínez-Vilalta, J., McDowell, N. G., Powers, J. S., Pugh, T. A., and Ruthrof, K. X.: Climate change risks to global forest health: emergence of unexpected events of elevated tree mortality worldwide, Annual Review of Plant Biology, 73, 673–702, publisher: Annual Reviews, 2022.

Hawkins, W. and Mittelstadt, B.: The ethical ambiguity of AI data enrichment: Measuring gaps in research ethics norms and practices, in: Proceedings of the 2023 ACM Conference on Fairness, Accountability, and Transparency, FAccT '23, pp. 261–270, Association for Computing Machinery, New York, NY, USA, https://doi.org/10.1145/3593013.3593995, 2023.

Hawryło, P., Bednarz, B., Wężyk, P., and Szostak, M.: Estimating defoliation of Scots pine stands using machine learning methods and vegetation indices of Sentinel-2, European Journal of Remote Sensing, 51, 194–204, https://doi.org/10.1080/22797254.2017.1417745, 2018.

Heinrich, V. H. A., Dalagnol, R., Cassol, H. L. G., Rosan, T. M., de Almeida, C. T., Silva Junior, C. H. L., Campanharo, W. A., House, J. I., Sitch, S., Hales, T. C., Adami, M., Anderson, L. O., and Aragão, L. E. O. C.: Large carbon sink potential of secondary forests in the Brazilian Amazon to mitigate climate change, Nature Communications, 12, 1785, https://doi.org/10.1038/s41467-021-22050-1, 2021.

Hicke, J. A., Allen, C. D., Desai, A. R., Dietze, M. C., Hall, R. J., Kashian, D. M., Moore, D., Raffa, K. F., Sturrock, R. N., Vogelmann, J., and others: Effects of biotic disturbances on forest carbon cycling in the United States and Canada, Global Change Biology, 18, 7–34, 2012.

Hicke, J. A., Meddens, A. J., and Kolden, C. A.: Recent Tree Mortality in the Western United States from Bark Beetles and Forest Fires, Forest Science, 62, 141–153, https://doi.org/10.5849/forsci.15-086, 2016.

Hicke, J. A., Xu, B., Meddens, A. J. H., and Egan, J. M.: Characterizing recent bark beetle-caused tree mortality in the western United States from aerial surveys, Forest Ecology and Management, 475, 118 402, https://doi.org/10.1016/j.foreco.2020.118402, 2020.

Imperatore, P.: SAR Imaging Distortions Induced by Topography: A Compact Analytical Formulation for Radiometric Calibration, Remote Sensing, 13, 3318, https://doi.org/10.3390/rs13163318, 2021.

https://doi.org/10.5194/egusphere-2025-4880
Preprint. Discussion started: 12 November 2025

Institute, C. B.: US Forest Service - FIA Forest Types of the Southeastern United States | Data Basin, https://databasin.org/datasets/e874a247b7e44693ad0792fb1a252aba/.

Jaccard, P.: Lois de distribution florale dans la zone alpine, https://doi.org/10.5169/SEALS-266762, 1902.

Jones, M. W., Abatzoglou, J. T., Veraverbeke, S., Andela, N., Lasslop, G., Forkel, M., Smith, A. J. P., Burton, C., Betts, R. A., van der Werf, G. R., Sitch, S., Canadell, J. G., Santín, C., Kolden, C., Doerr, S. H., and Le Quéré, C.: Global and Regional Trends and Drivers of Fire Under Climate Change, Reviews of Geophysics, 60, e2020RG000726, https://doi.org/10.1029/2020RG000726, 2022.

Justice, C., Vermote, E., Townshend, J., Defries, R., Roy, D., Hall, D., Salomonson, V., Privette, J., Riggs, G., Strahler, A., Lucht, W., Myneni, R., Knyazikhin, Y., Running, S., Nemani, R., Wan, Z., Huete, A., van Leeuwen, W., Wolfe, R., Giglio, L., Muller, J., Lewis, P., and Barnsley, M.: The Moderate Resolution Imaging Spectroradiometer (MODIS): land remote sensing for global change research, IEEE Transactions on Geoscience and Remote Sensing, 36, 1228–1249, https://doi.org/10.1109/36.701075, 1998.

Kautz, M.: On correcting the time-lag bias in aerial-surveyed bark beetle infestation data, Forest Ecology and Management, 326, 157–162, https://doi.org/10.1016/j.foreco.2014.04.010, 2014.

Kautz, M., Meddens, A. J. H., Hall, R. J., and Arneth, A.: Biotic disturbances in Northern Hemisphere forests-a synthesis of recent data, uncertainties and implications for forest monitoring and modelling, Global Ecology and Biogeography, 26, 533–552, https://doi.org/10.1111/geb.12558, 2017.

Kautz, M., Anthoni, P., Meddens, A. J. H., Pugh, T. A. M., and Arneth, A.: Simulating the recent impacts of multiple biotic disturbances on forest carbon cycling across the United States, Global Change Biology, 24, 2079–2092, https://doi.org/10.1111/gcb.13974, 2018.

Konings, A. G., Saatchi, S. S., Frankenberg, C., Keller, M., Leshyk, V., Anderegg, W. R. L., Humphrey, V., Matheny, A. M., Trugman, A., Sack, L., Agee, E., Barnes, M. L., Binks, O., Cawse-Nicholson, K., Christoffersen, B. O., Entekhabi, D., Gentine, P., Holtzman, N. M., Katul, G. G., Liu, Y., Longo, M., Martinez-Vilalta, J., McDowell, N., Meir, P., Mencuccini, M., Mrad, A., Novick, K. A., Oliveira, R. S., Siqueira, P., Steele-Dunne, S. C., Thompson, D. R., Wang, Y., Wehr, R., Wood, J. D., Xu, X., and Zuidema, P. A.: Detecting forest response to droughts with global observations of vegetation water content, Global Change Biology, 27, 6005–6024, https://doi.org/10.1111/gcb.15872, _eprint: https://onlinelibrary.wiley.com/doi/pdf/10.1111/gcb.15872, 2021.

Korosuo, A., Pilli, R., Abad Viñas, R., Blujdea, V. N. B., Colditz, R. R., Fiorese, G., Rossi, S., Vizzarri, M., and Grassi, G.: The role of forests in the EU climate policy: are we on the right track?, Carbon Balance and Management, 18, 15, https://doi.org/10.1186/s13021-023-00234-0, 2023.

Kurz, W. A., Dymond, C. C., Stinson, G., Rampley, G. J., Neilson, E. T., Carroll, A. L., Ebata, T., and Safranyik, L.: Mountain pine beetle and forest carbon feedback to climate change, Nature, 452, 987–990, https://doi.org/10.1038/nature06777, 2008.

Markham, B. L. and Helder, D. L.: Forty-year calibrated record of earth-reflected radiance from Landsat: A review, Remote Sensing of Environment, 122, 30–40, https://doi.org/10.1016/j.rse.2011.06.026, 2012.

McConnell, T. J.: A Guide to Conducting Aerial Sketchmapping Surveys, U.S. Department of Agriculture, Forest Service, Forest Health Technology Enterprise Team, google-Books-ID: PQ0UAAAAYAAJ, 2000.

McDowell, N. G., Coops, N. C., Beck, P. S., Chambers, J. Q., Gangodagamage, C., Hicke, J. A., Huang, C.-y., Kennedy, R., Krofcheck, D. J., Litvak, M., Meddens, A. J., Muss, J., Negrón-Juarez, R., Peng, C., Schwantes, A. M., Swenson, J. J., Vernon, L. J., Williams, A. P., Xu, C., Zhao, M., Running, S. W., and Allen, C. D.: Global satellite monitoring of climate-induced vegetation disturbances, Trends in Plant Science, 20, 114–123, http://www.sciencedirect.com/science/article/pii/S1360138514002726, 2015.

McDowell, N. G., Allen, C. D., Anderson-Teixeira, K., Aukema, B. H., Bond-Lamberty, B., Chini, L., Clark, J. S., Dietze, M., Grossiord, C., Hanbury-Brown, A., Hurtt, G. C., Jackson, R. B., Johnson, D. J., Kueppers, L., Lichstein, J. W., Ogle, K., Poulter, B., Pugh, T. A. M.,

https://doi.org/10.5194/egusphere-2025-4880
Preprint. Discussion started: 12 November 2025

Seidl, R., Turner, M. G., Uriarte, M., Walker, A. P., and Xu, C.: Pervasive shifts in forest dynamics in a changing world, Science, 368, eaaz9463, https://doi.org/10.1126/science.aaz9463, 2020.

Meddens, A. J. H., Hicke, J. A., and Ferguson, C. A.: Spatiotemporal patterns of observed bark beetle-caused tree mortality in British Columbia and the western United States, Ecological Applications, 22, 1876–1891, 2012.

Nabuurs, G.-J., Lindner, M., Verkerk, H., Gunia, K., Deda, P., Michalak, R., and Grassi, G.: First signs of carbon sink saturation in European forest biomass, Nature Climate Change, 3, https://doi.org/10.1038/nclimate1853, 2013.

Negrón-Juárez, R. I., Holm, J. A., Marra, D. M., Rifai, S. W., Riley, W. J., Chambers, J. Q., Koven, C. D., Knox, R. G., McGroddy, M. E., Vittorio, A. V. D., Urquiza-Muñoz, J., Tello-Espinoza, R., Muñoz, W. A., Ribeiro, G. H. P. M., and Higuchi, N.: Vulnerability of Amazon forests to storm-driven tree mortality, Environmental Research Letters, 13, 054 021, https://doi.org/10.1088/1748-9326/aabe9f, 2018.

Pan, Y., Birdsey, R. A., Phillips, O. L., Houghton, R. A., Fang, J., Kauppi, P. E., Keith, H., Kurz, W. A., Ito, A., Lewis, S. L., Nabuurs, G.-J., Shvidenko, A., Hashimoto, S., Lerink, B., Schepaschenko, D., Castanho, A., and Murdiyarso, D.: The enduring world forest carbon sink, Nature, 631, 563–569, https://doi.org/10.1038/s41586-024-07602-x, number: 8021 Publisher: Nature Publishing Group, 2024.

Patacca, M., Schelhaas, M.-J., Zudin, S., and Lindner, M.: Database on Forest Disturbances in Europe (DFDE)-Technical report History, State of the Art, and Future Perspectives, Project I-Maestro (ERA-NET Cofund ForestValue), 2021.

PBC, P. L.: Education and Research Program | Planet, https://www.planet.com/industries/education-and-research/.

Popp, T., Hegglin, M. I., Hollmann, R., Ardhuin, F., Bartsch, A., Bastos, A., Bennett, V., Boutin, J., Brockmann, C., Buchwitz, M., Chuvieco, E., Ciais, P., Dorigo, W., Ghent, D., Jones, R., Lavergne, T., Merchant, C. J., Meyssignac, B., Paul, F., Quegan, S., Sathyendranath, S., Scanlon, T., Schröder, M., Simis, S. G. H., and Willén, U.: Consistency of Satellite Climate Data Records for Earth System Monitoring, Bulletin of the American Meteorological Society, 101, E1948–E1971, https://doi.org/10.1175/BAMS-D-19-0127.1, 2020.

Richter, R., Ballasus, H., Engelmann, R. A., Zielhofer, C., Sanaei, A., and Wirth, C.: Tree species matter for forest microclimate regulation during the drought year 2018: disentangling environmental drivers and biotic drivers, Scientific Reports, 12, 17 559, https://doi.org/10.1038/s41598-022-22582-6, 2022.

Rüetschi, M., Small, D., and Waser, L. T.: Rapid Detection of Windthrows Using Sentinel-1 C-Band SAR Data, Remote Sensing, 11, 115, https://doi.org/10.3390/rs11020115, 2019.

Schuldt, B., Buras, A., Arend, M., Vitasse, Y., Beierkuhnlein, C., Damm, A., Gharun, M., Grams, T. E. E., Hauck, M., Hajek, P., Hartmann, H., Hiltbrunner, E., Hoch, G., Holloway-Phillips, M., Körner, C., Larysch, E., Lübbe, T., Nelson, D. B., Rammig, A., Rigling, A., Rose, L., Ruehr, N. K., Schumann, K., Weiser, F., Werner, C., Wohlgemuth, T., Zang, C. S., and Kahmen, A.: A first assessment of the impact of the extreme 2018 summer drought on Central European forests, Basic and Applied Ecology, 45, 86–103, https://doi.org/10.1016/j.baae.2020.04.003, 2020.

Seidl, R. and Turner, M. G.: Post-disturbance reorganization of forest ecosystems in a changing world, Proceedings of the National Academy of Sciences, 119, e2202190 119, https://doi.org/10.1073/pnas.2202190119, publisher: Proceedings of the National Academy of Sciences, 2022.

Seidl, R., Schelhaas, M.-J., Rammer, W., and Verkerk, P. J.: Increasing forest disturbances in Europe and their impact on carbon storage, Nature climate change, 4, 806–810, 2014.

Seidl, R., Thom, D., Kautz, M., Martin-Benito, D., Peltoniemi, M., Vacchiano, G., Wild, J., Ascoli, D., Petr, M., Honkaniemi, J., Lexer, M. J., Trotsiuk, V., Mairota, P., Svoboda, M., Fabrika, M., Nagel, T. A., and Reyer, C. P.: Forest disturbances under climate change, Nature Climate Change, 7, 395–402, https://doi.org/10.1038/NCLIMATE3303, publisher: Nature Publishing Group, 2017.

https://doi.org/10.5194/egusphere-2025-4880
Preprint. Discussion started: 12 November 2025

Senf, C. and Seidl, R.: Natural disturbances are spatially diverse but temporally synchronized across temperate forest landscapes in Europe, Global Change Biology, 24, 1201–1211, https://doi.org/10.1111/gcb.13897, publisher: John Wiley & Sons, Ltd, 2018.

Senf, C. and Seidl, R.: Persistent impacts of the 2018 drought on forest disturbance regimes in Europe, Biogeosciences, 18, 5223–5230, https://doi.org/10.5194/bg-18-5223-2021, 2021a.

Senf, C. and Seidl, R.: Storm and fire disturbances in Europe: Distribution and trends, Global Change Biology, 27, 3605–3619, https://doi.org/10.1111/gcb.15679, _eprint: https://onlinelibrary.wiley.com/doi/pdf/10.1111/gcb.15679, 2021b.

Senf, C., Pflugmacher, D., Wulder, M. A., and Hostert, P.: Characterizing spectral–temporal patterns of defoliator and bark beetle disturbances using Landsat time series, Remote Sensing of Environment, 170, 166–177, https://doi.org/10.1016/j.rse.2015.09.019, 2015.

Senf, C., Müller, J., and Seidl, R.: Post-disturbance recovery of forest cover and tree height differ with management in Central Europe, Landscape Ecology, 34, 2837–2850, https://doi.org/10.1007/s10980-019-00921-9, 2019.

Senf, C., Buras, A., Zang, C. S., Rammig, A., and Seidl, R.: Excess forest mortality is consistently linked to drought across Europe, Nature Communications, 11, 6200, https://doi.org/10.1038/s41467-020-19924-1, 2020.

Small, D.: Flattening Gamma: Radiometric Terrain Correction for SAR Imagery, IEEE Transactions on Geoscience and Remote Sensing, 49, 3081–3093, https://doi.org/10.1109/TGRS.2011.2120616, 2011.

Thom, D. and Seidl, R.: Natural disturbance impacts on ecosystem services and biodiversity in temperate and boreal forests, Biological Reviews, 91, 760–781, https://doi.org/10.1111/brv.12193, 2016.

Trumbore, S., Brando, P., and Hartmann, H.: Forest health and global change, Science, 349, 814–818, https://doi.org/10.1126/science.aac6759, 2015.

Vicente-Serrano, S. M., Gouveia, C., Camarero, J. J., Beguería, S., Trigo, R., López-Moreno, J. I., Azorín-Molina, C., Pasho, E., Lorenzo-Lacruz, J., Revuelto, J., Morán-Tejeda, E., and Sanchez-Lorenzo, A.: Response of vegetation to drought time-scales across global land biomes, Proceedings of the National Academy of Sciences, 110, 52–57, https://doi.org/10.1073/pnas.1207068110, 2013.

Wagner, W., Bauer-Marschallinger, B., Navacchi, C., Reuß, F., Cao, S., Reimer, C., Schramm, M., and Briese, C.: A Sentinel-1 Backscatter Datacube for Global Land Monitoring Applications, Remote Sensing, 13, 4622, https://doi.org/10.3390/rs13224622, 2021.

Winkler, K., Yang, H., Ganzenmüller, R., Fuchs, R., Ceccherini, G., Duveiller, G., Grassi, G., Pongratz, J., Bastos, A., Shvidenko, A., Araza, A., Herold, M., Wigneron, J.-P., and Ciais, P.: Changes in land use and management led to a decline in Eastern Europe's terrestrial carbon sink, Communications Earth & Environment, 4, 1–14, https://doi.org/10.1038/s43247-023-00893-4, 2023.